



Doc n°: IA-RP-2000-4332-CNE
Issue: 1.0
Date: 2017-07-25
Sheet: 1 Of: 60

IASI QUARTERLY PERFORMANCE REPORT
FROM 2016/12/01 TO 2017/02/28

BY IASI TEC (TECHNICAL EXPERTISE CENTER)
FOR IASI PFM-R ON METOP B



Doc n°: IA-RP-2000-4332-CNE

Issue: 1.0

Date: 2017-07-25

Sheet: 2 Of: 60

ANALYSE DOCUMENTAIRE**Bordereau d'indexation**

| | | | |
|--|--|------------------------------------|--------------------------------|
| | | | |
| Mots clés d'auteur : IASI TEC quarterly synthesis report | | | |
| OBJET : IASI TEC periodic report | | | |
| TITRE : IASI quarterly performance report | | | |
| | | | |
| RESUME : Quarterly report issued by the IASI TEC team to show trends and layout from the "long term synthesis" TEC function for flags and observables quality indicators | | | |
| | | | |
| Volume : 1 | Nombre de pages total : 60 dont - liminaires : 7 annexes : 0 | Nombre d'annexes : 0 | LANGUE : English |
| | | | |
| | | | |
| | | | |

| | | |
|---|---|--|
|  |  | Doc n°: IA-RP-2000-4332-CNE Issue: 1.0 Date: 2017-07-25 Sheet: 3 Of: 60 |
|---|---|--|

DIFFUSION

On CNES web site : <https://iasi.cnes.fr>
Instrument characteristics / In-orbit performances monitoring

DOCUMENT MODEL CHANGE RECORD

| Version | Date | Paragraphs | Description |
|----------------|-------------|-----------------------|--|
| 1.0 | 05/03/11 | | Creation of the model |
| 2.0 | 01/01/15 | 4.3.2.5 4.8 | Cube corner Speed Quality (CSQ) monitoring IASI-B inter-calibration with IASI-A, CRIS and AIRS |
| 2.1 | 01/03/16 | 4.6.2 4.6.3 4.9 | Spectral calibration will be synthesized only once per year (in REVEX report) Monitoring of the Ghost evolution is stopped (there is no more ghost since CD stop) IIS noise and IIS radiometric calibration will be computed in one monthly external calibration in three and monitored only once per year (in REVEX report) |

DOCUMENT CHANGE RECORD

| Version | Date | Paragraphs | Description |
|----------------|-------------|-------------------|--------------------------|
| 1.0 | 2017-07-25 | | Creation of the document |
| | | | |

| | | |
|---|---|-----------------------------|
|  |  | Doc n°: IA-RP-2000-4332-CNE |
| | | Issue: 1.0 |
| | | Date: 2017-07-25 |
| | | Sheet: 4 Of: 60 |

Table of contents

| | |
|---|-----------|
| 1 INTRODUCTION..... | 9 |
| 2 RELATED DOCUMENTS..... | 9 |
| 2.1 APPLICABLE DOCUMENTS..... | 9 |
| 2.2 REFERENCE DOCUMENTS..... | 9 |
| 3 SIGNIFICANT EVENTS..... | 10 |
| 3.1 EXTERNAL CALIBRATION..... | 10 |
| 3.2 ON BOARD CONFIGURATION..... | 11 |
| 3.3 GROUND CONFIGURATIONS UPDATES FOR LEVEL 1 PROCESSING..... | 11 |
| 3.4 DATA BASES UPDATE FOR THE USERS..... | 12 |
| 3.5 ON GROUND HW/SW EVOLUTION..... | 12 |
| 3.6 DECONTAMINATION..... | 13 |
| 3.7 INSTRUMENT..... | 13 |
| 3.7.1 External events..... | 13 |
| 3.7.2 Operation leading to mission outage..... | 13 |
| 3.7.3 Anomaly leading to mission outage..... | 14 |
| 4 PERFORMANCE MONITORING..... | 15 |
| 4.1 PERFORMANCE MONITORING..... | 15 |
| 4.2 PERFORMANCE SYNOPSIS..... | 16 |
| 4.3 LEVEL 0 DATA QUALITY (L0)..... | 17 |
| 4.3.1 Overall quality..... | 17 |
| 4.3.2 Main flag and quality indicator parameters..... | 19 |
| 4.3.3 Second level flags and quality indicators..... | 28 |
| 4.3.4 Conclusion..... | 28 |
| 4.4 LEVEL 1 DATA QUALITY (L1)..... | 29 |
| 4.4.1 Overall quality..... | 29 |
| 4.4.2 Main flag and quality indicator parameters..... | 30 |
| 4.4.3 Conclusion..... | 33 |
| 4.5 SOUNDER RADIOMETRIC PERFORMANCES..... | 34 |
| 4.5.1 Radiometric Noise..... | 34 |
| 4.5.2 Radiometric Calibration..... | 35 |
| 4.5.3 Delay of Detection Chains..... | 39 |
| 4.5.4 Optical Transmission..... | 40 |
| 4.5.5 Interferometric Contrast..... | 42 |
| 4.5.6 Interferogram Baseline..... | 43 |
| 4.5.7 Detection Chain..... | 44 |
| 4.5.8 Conclusion..... | 44 |
| 4.6 SOUNDER SPECTRAL PERFORMANCES..... | 45 |
| 4.6.1 Monitoring of the ISRF inputs..... | 45 |
| 4.6.2 Spectral calibration assessment..... | 47 |
| 4.6.3 Conclusion..... | 47 |
| 4.7 GEOMETRIC PERFORMANCES..... | 48 |
| 4.7.1 Sounder / IIS co-registration monitoring..... | 48 |
| 4.7.2 IIS / AVHRR co-registration..... | 48 |
| 4.7.3 Conclusion..... | 49 |

| | | |
|---|---|-----------------------------|
|  |  | Doc n°: IA-RP-2000-4332-CNE |
| | | Issue: 1.0 |
| | | Date: 2017-07-25 |
| | | Sheet: 5 Of: 60 |

| | |
|--|-----------|
| 4.8 IASI-B INTER-CALIBRATION WITH IASI-A, CRIS AND AIRS..... | 50 |
| 4.8.1 IASI-B inter-calibration with IASI-A..... | 50 |
| 4.8.2 IASI-B inter-calibration with CRIS..... | 53 |
| 4.8.3 IASI-B inter-calibration with AIRS..... | 55 |
| 4.9 IIS RADIOMETRIC PERFORMANCES..... | 57 |
| 4.9.1 IIS Radiometric Noise Monitoring..... | 57 |
| 4.9.2 IIS Radiometric Calibration Monitoring..... | 57 |
| 5 IASI TEC SOFTWARE AND INTERFACES..... | 58 |
| 5.1 IASI TEC EVOLUTION..... | 58 |
| 5.2 SIC EVOLUTION..... | 58 |
| 5.3 EUMETCAST INTERFACE..... | 59 |
| 5.4 FTP INTERFACE..... | 59 |
| 6 CONCLUSION AND OPERATIONS FORESEEN..... | 60 |
| 6.1 SUMMARY..... | 60 |
| 6.2 SHORT-TERM EVENTS..... | 60 |
| 6.3 OPERATIONS FORESEEN..... | 60 |

Figures and tables

| | |
|--|----|
| Table 1: External Calibration TEC Requests..... | 10 |
| Table 2: DPS and MAS configuration TEC Requests..... | 11 |
| Table 3: DPS and MAS previous configuration..... | 11 |
| Table 4: IASI L1 Auxiliary File Configuration on the Operational EPS Ground Segment..... | 11 |
| Table 5: IASI L1 auxiliary file previous configuration..... | 11 |
| Table 6: IASI Data Bases for the users..... | 12 |
| Table 7: previous IASI Data Bases..... | 12 |
| Table 8: IASI L1 PPF Configuration on the Operational EPS Ground Segment..... | 12 |
| Table 9: Previous IASI L1 PPF..... | 12 |
| Table 10: Decontamination TEC Requests..... | 13 |
| Table 11: Previous decontamination..... | 13 |
| Table 12: Overview of METOP manoeuvres in the reporting period..... | 13 |
| Table 13: PL-SOL..... | 13 |
| Table 14: Scheduled interruptions..... | 13 |
| Table 15: Major anomalies..... | 14 |
| Table 16: Minor anomalies..... | 14 |
| Table 17: Functional status legend | 15 |
| Table 18: IASI product components functional status | 16 |
| Figure 1 : IASI L0 data quality orbit average (per pixel and CCD)..... | 17 |
| Figure 2 : IASI L0 data quality spatial distribution (per pixel)..... | 18 |
| Figure 3 : Temporal evolution of spikes anomaly ratio in % for all pixels (orbit average)..... | 19 |
| Figure 4 : Geographical distribution of spikes occurrences in % for band 3 and all pixels..... | 20 |
| Figure 5 : Temporal evolution of NZPD determination anomaly ratio in % for all pixels (orbit average)..... | 21 |
| Figure 6 : IASI NZPD determination quality flag spatial distribution (per pixel)..... | 22 |
| Figure 7 : NZPD inter-pixel for all pixels and CCD calculated with respect to pixel 1 (orbit average)..... | 23 |
| Figure 8 : IASI L0 over/under-flows orbit average of all pixels..... | 24 |
| Figure 9 : IASI Overflows and Underflows spatial distribution (per pixel)..... | 25 |

| | | |
|---|---|-----------------------------|
|  |  | Doc n°: IA-RP-2000-4332-CNE |
| | | Issue: 1.0 |
| | | Date: 2017-07-25 |
| | | Sheet: 6 Of: 60 |

| | |
|---|----|
| Figure 10 : Max of NZPD quality index for all pixels and CCD - BB..... | 26 |
| Figure 11 : Max of NZPD quality index for all pixels and CCD - CS..... | 27 |
| Figure 12 : Number of CSQ..... | 28 |
| Figure 14 : IASI product overall quality spatial distribution (per pixel)..... | 30 |
| Figure 15 : GQisQualIndex average (L1 data quality index for IASI sounder)..... | 31 |
| Figure 16 : GQisQualIndexIIS average (L1 data quality index for IASI Integrated Imager)..... | 31 |
| Figure 17 : GQisQualIndexSpect average (L1 data index for spectral calibration quality)..... | 32 |
| Figure 18 : GQisQualIndexRad average (L1 data index for radiometric calibration quality)..... | 32 |
| Figure 19 : GQisQualIndexLoc average (L1 data index for ground localisation quality)..... | 33 |
| Figure 20 : MDptPixQual average (L1 quality index for IASI integrated imager, fraction of not dead pixels)..... | 33 |
| Figure 21 : Instrument noise evolution between start and end of the period..... | 34 |
| Figure 22 : Scan mirror reflectivity evolution..... | 35 |
| Figure 23 : Radiometric calibration error due to scan mirror reflectivity dependency with viewing angle Maximum effect on SN1 for different scene temperature. Done with the period May 16 / Feb 17..... | 36 |
| Figure 24 : Black Body Temperature..... | 37 |
| Figure 25 : Focal Plane Temperature..... | 38 |
| Figure 26 : Monitoring of detection chain maximum delays for all bands..... | 39 |
| Figure 27 : Ratio of calibration coefficient slopes as a function of wave number and time after the last decontamination..... | 40 |
| Figure 28 : Temporal evolution of calibration ratio coefficient slopes since the last decontamination. The curve was fitted with a decreasing exponential function to determine a rough date for the next decontamination (relative gain evolution of 0.8) | 41 |
| Figure 29 : Contrast Monitoring..... | 42 |
| Figure 30 : Monitoring of interferogram baseline..... | 43 |
| Figure 31 : Monitoring of detection chain margins..... | 44 |
| Figure 32 : GFaxAxeY average (Y filtered coordinates of sounder interferometric axis)..... | 45 |
| Figure 33 : GFaxAxeZ average (Z filtered coordinates of sounder interferometric axis)..... | 46 |
| Figure 34 : Cube Corner offset variation..... | 46 |
| Figure 35 : Optical bench Temperature..... | 47 |
| Figure 36 : Column offset (black) guess vs. column offset averaged over all lines (LN) as a function of the scan position (SP=SN), and orbit number..... | 48 |
| Figure 37 : Line offset guess (black) vs. line offset averaged over all lines (LN) as a function of the scan position (SP=SN), and the orbit number..... | 49 |
| Figure 38 : Mean (black curve) and standard deviation (yellow) of the difference in brightness temperature IASI-B – IASI-A..... | 50 |
| Figure 39 : Temporal evolution of differences IASI-B – IASI-A in brightness temperature spectrally integrated over the approximate three IASI bands..... | 51 |
| Figure 40 : Mean (black curve) and standard deviation (yellow curve) of the difference spectral calibration $\Delta v/v$ between IASI-B and A..... | 52 |
| Figure 41 : Temporal evolution of the difference spectral calibration $\Delta v/v$ between IASI-B and A in the spectral window centered around 2200cm ⁻¹ | 52 |
| Figure 42 : Mean (black curve) and standard deviation (yellow) of the difference in brightness temperature IASI-B – CRIS..... | 53 |
| Figure 43 : Temporal evolution of the differences IASI-B – CRIS in brightness temperature over the approximate three IASI bands, with monthly means..... | 54 |
| Figure 44 : Mean (black curve) and standard deviation (yellow) of the difference in brightness temperature IASI-B – AIRS..... | 55 |
| Figure 45 : Temporal evolution of the differences IASI-B – AIRS in brightness temperature over the approximate three IASI bands, with monthly mean..... | 56 |
| Table 19: IASI TEC at CNES Toulouse..... | 58 |
| Table 20: SIC at CNES Toulouse..... | 58 |
| Table 21: EUMETCAST configuration at CNES Toulouse..... | 59 |

| | | |
|---|---|--|
|  |  | Doc n°: IA-RP-2000-4332-CNE Issue: 1.0 Date: 2017-07-25 Sheet: 7 Of: 60 |
|---|---|--|

| |
|------------------|
| LIST OF ACRONYMS |
|------------------|

| | |
|-----------|---|
| 4A/OP | Automatized Atmospheric Absorptions Atlas/ Operational |
| APO | Other Parameters OPS |
| AR | Anomaly Report |
| ASE | Acquisition Start End |
| AVHRR | Advanced Very High Resolution Radiometer |
| BB | Black Body |
| BRD | BoaRD configuration |
| CCFD | Cube Corner Functional Device |
| CCD | Cube Corner Direction |
| CCM | Cube Corner Mechanism |
| CD | Cube corner Compensation Device |
| CHART | Component Health Assessment and Reporting Tool |
| CGS | Core Ground Segment at EUMETSAT |
| CNES | Centre National d'Etudes Spatiales |
| CS | Cold Space |
| DA | Applicable document |
| DPS | Data Processing Subsystem |
| ECMWF | European Centre for Medium Range Weather Forecasts |
| EM | Engineering Model |
| EPS | EUMETSAT Polar System |
| EUMETSAT | European organisation for exploitation of METeorological SATellites |
| FM2 / FM3 | Flight Model n°2 or 3 |
| FOV | Field Of View |
| GRD | GRounD configuration |
| IASI | Infrared Atmospheric Sounding Interferometer |
| IIS | Integrated Imaging Subsystem |
| IPSF | Instrument Point Spread Function |
| ISRF | Instrument Spectral Response Function |
| LFD | Locking Filtering Device |
| LN | Line Number |
| LSB | Least Significant Bit |
| METOP | METeorological OPerational satellite |
| MPF | Mission Planning Facility |
| NedT | Noise equivalent difference Temperature |
| NDVI | Normalized Difference Vegetation Index |
| NZPD | Number of Zero Path Difference |
| ODB | Operational Data Base |
| OPS | Operational Software |
| PC | Principal Component |
| PDD | Position Data Diagnostic |

| | | |
|---|---|--|
|  |  | Doc n°: IA-RP-2000-4332-CNE Issue: 1.0 Date: 2017-07-25 Sheet: 8 Of: 60 |
|---|---|--|

| | |
|--------|--|
| PDU | Product Dissemination Unit |
| PL SOL | PayLoad Switch Off-Line |
| PN | Pixel Number |
| PTSI | Parameter Table Status Identifier |
| RMS | Root Mean Square |
| RD | Reference Document |
| SAA | South Atlantic Anomaly |
| SEU | Single Event Upset |
| TEC | IASI Technical Centre of Expertise (located in CNES, Toulouse) |
| TIGR | Thermodynamic Initial Guess Retrieval data set |
| VDS | Verification Data Selection |
| ZPD | Zero Path Difference |

| | | |
|---|---|--|
|  |  | Doc n°: IA-RP-2000-4332-CNE Issue: 1.0 Date: 2017-07-25 Sheet: 9 Of: 60 |
|---|---|--|

1 INTRODUCTION

The IASI TEC is based at CNES Toulouse and is responsible for the monitoring of the IASI system performances, covering both instrument and level 1 processing sub-system.

This document describes the activities and results obtained at the IASI TEC for instrument PFM-R on METOP-B during the following period:

- Start Time: 2016/12/01 Orbit: 21812
- End Time: 2017/02/28 Orbit: 23090
- Duration: 3 months

Note that IASI ended the Calibration / Validation (commissioning) phase on April 2013.

2 RELATED DOCUMENTS

| | | |
|---|---|---|
|  |  | Doc n°: IA-RP-2000-4332-CNE Issue: 1.0 Date: 2017-07-25 Sheet: 10 Of: 60 |
|---|---|---|

3 SIGNIFICANT EVENTS

The following tables present a timeline of the various requests sent by TEC and the external IASI activities.

Those events are typically the configuration changes, programming requests, software update, but also any external operation or activity such as mission interruption, manoeuvre, dissemination problem, ...

3.1 EXTERNAL CALIBRATION

Table 1 shows the External Calibration within the time period reported here. Note that the VDS files that come with each request are not described here.

| Execution | TEC ref. ⁽¹⁾ | Description | Activities |
|---|-------------------------|--|--|
| 02/12/2016 from 5h16 to 9h12 orb. 21829 to 21831 | RM-46 | Monthly_MPF ⁽²⁾ Targets: Earth 15, Blackbody, 2 nd Deep Space, Mirror Backside | For routine monitoring (IIS and IASI NeDT, scan mirror reflectivity, ghost,...) |
| From 17/12/2016 11h10 to 18/12/2016 10h25 orb. 22046 to 22059 | RL-16 | Moon avoidance MPF ⁽²⁾ Targets: 1 st Deep Space | Monitoring of moon intrusion in CS1 FOV |
| 31/12/2016 from 5h16 to 9h12 orb. 22241 to 22243 | RM-47 | Monthly_MPF ⁽²⁾ Targets: Earth 15, Blackbody, 2 nd Deep Space, Mirror Backside | For routine monitoring (IIS and IASI NeDT, scan mirror reflectivity, ghost,...) |
| From 15/01/2017 21h04 to 16/01/2017 22h29 orb. 22464 to 22479 | RL-17 | Moon avoidance MPF ⁽²⁾ Targets: 1 st Deep Space | Monitoring of moon intrusion in CS1 FOV |
| 29/01/2017 from 5h16 to 9h12 orb. 22653 to 22655 | RM-48 | Monthly_MPF ⁽²⁾ Targets: Earth 15, Blackbody, 2 nd Deep Space, Mirror Backside | For routine monitoring (IIS and IASI NeDT, scan mirror reflectivity, ghost,...) |
| 27/02/2017 from 5h16 to 9h12 orb. 23065 to 23067 | RM-49 | Monthly_MPF ⁽²⁾ Targets: Earth 15, Blackbody, 2 nd Deep Space, Mirror Backside | For routine monitoring (IIS and IASI NeDT, scan mirror reflectivity, ghost,...) |

Table 1: External Calibration TEC Requests

⁽¹⁾ TEC convention: R for Routine, M for Monthly and L for moon avoidance, followed by a chronological number

⁽²⁾ An external calibration could be the result of:

- a TEC request or
- a “MPF” uploaded directly by EUMETSAT in full accordance with TEC. The reference “Monthly_MPF” is based on the March 2008 TEC External Calibration request. The MPF for moon avoidance is based on the December 2008 TEC External Calibration request: “ICAL_OCF_xx_M02_20081216060000Z_20090616060000Z_20081209100934Z_IAST_EXTCALIBRA.dts”

Moon external calibration RL-16 detail:

| External Calibration | | External Calibration | |
|----------------------|----------|----------------------|----------|
| from | to | from | to |
| 2016/12/17 11:10:42 | 11:34:57 | 2016/12/17 23:10:10 | 00:11:45 |
| 2016/12/17 12:51:30 | 13:19:29 | 2016/12/18 01:14:26 | 01:56:01 |
| 2016/12/17 14:32:02 | 15:05:05 | 2016/12/18 03:01:06 | 03:40:01 |
| 2016/12/17 16:13:22 | 17:04:01 | 2016/12/18 04:46:26 | 05:21:53 |
| 2016/12/17 17:57:22 | 18:59:45 | 2016/12/18 06:32:50 | 07:02:57 |
| 2016/12/17 19:41:38 | 20:43:29 | 2016/12/18 08:17:54 | 08:44:01 |
| 2016/12/17 21:25:54 | 22:27:29 | 2016/12/18 10:02:10 | 10:25:05 |

| | | |
|---|---|-----------------------------|
|  |  | Doc n°: IA-RP-2000-4332-CNE |
| | | Issue: 1.0 |
| | | Date: 2017-07-25 |
| | | Sheet: 11 Of: 60 |

Moon external calibration RL-17 detail:

| External Calibration | | External Calibration | |
|----------------------|----------|----------------------|----------|
| from | to | from | to |
| 2017/01/15 21:04:45 | 21:29:48 | 2017/01/16 10:19:09 | 10:51:08 |
| 2017/01/15 22:44:13 | 23:14:36 | 2017/01/16 11:58:53 | 12:30:20 |
| 2017/01/16 00:23:57 | 00:54:52 | 2017/01/16 13:38:37 | 14:09:48 |
| 2017/01/16 02:03:09 | 02:34:36 | 2017/01/16 15:18:37 | 15:49:16 |
| 2017/01/16 03:42:21 | 04:14:04 | 2017/01/16 16:58:53 | 17:28:44 |
| 2017/01/16 05:21:33 | 05:53:32 | 2017/01/16 18:39:09 | 19:08:44 |
| 2017/01/16 07:01:01 | 07:32:44 | 2017/01/16 20:19:41 | 20:48:44 |
| 2017/01/16 08:39:57 | 09:11:56 | 2017/01/16 22:05:33 | 22:29:00 |

3.2 ON BOARD CONFIGURATION

Table 2 presents the on-board processing configuration updates that had been made within the time period reported here:

| PTSI | IASI on board parameter files | Delivery by TEC | activated on | TEC ref. | affected parameters of a DPS TOP configuration update |
|------|-------------------------------|-----------------|--------------|----------|---|
| | | | | | |

Table 2: DPS and MAS configuration TEC Requests

For information, Table 3 shows the delivery applicable at the beginning of the period:

| PTSI | IASI on board parameter files | Delivery by TEC | activated on | TEC ref. | affected parameters of a DPS TOP configuration update |
|-----------|---|-----------------|----------------------------|----------|---|
| 11 1.0 | IDPS_OBP_xx_M01_2015020900000Z_2015080900000Z_20150206092603Z_IAST_DPSPARAMOD.tar | 06/02/2015 | 19/02/2015, orbit 12572 | R_41 | Update of reduced spectra |

Table 3: DPS and MAS previous configuration

The associated ground configuration table (BRD file), necessary to handle coherent configuration at system level, is presented in the next section. These associated configuration table are necessary for L1 processing.

3.3 GROUND CONFIGURATIONS UPDATES FOR LEVEL 1 PROCESSING

Table 4 presents the on-ground processing configuration updates that had been made within the time period reported here:

| IDef | IASI L1 auxiliary files | Delivery by TEC | Upload on GS1 | Content |
|------|-------------------------|-----------------|---------------|---------|
| | | | | |

Table 4: IASI L1 Auxiliary File Configuration on the Operational EPS Ground Segment

For information, Table 5 shows the delivery applicable at the beginning of the period:

| IDef | IASI L1 auxiliary files | Delivery by TEC | Upload on GS1 | Content |
|------|---|-----------------|--|------------------------------------|
| 42 | IASI_BRD_xx_M01_2016060100000Z_xxxx_xxxxxxxZ_20160525091317Z_IAST_00000001 | 25/05/2016 | BRD and GRD activated on 28/06/2016 11:56, orbit 19603 | Update of Scan Mirror Reflectivity |
| 21 | IASI_GRD_xx_M01_2016060100000Z_xxxx_xxxxxxxZ_20160525091327Z_IAST_000000021 | | | |
| 12 | IASI_ODB_xx_M01_2013041710000Z_xxxx_xxxxxxxZ_20130417082506Z_IAST_000000012 | 17/04/13 | ODB activated on 14/05/13 12:05 orbit 3393 | |

Table 5: IASI L1 auxiliary file previous configuration

| | | |
|---|---|-----------------------------|
|  |  | Doc n°: IA-RP-2000-4332-CNE |
| | | Issue: 1.0 |
| | | Date: 2017-07-25 |
| | | Sheet: 12 Of: 60 |

3.4 DATA BASES UPDATE FOR THE USERS

The Noise Covariance Matrix (NCM) and Spectral data base (SDB) are specific data bases for the users. They are updated according to the main ground level 1 evolutions.

Table 6 presents the updates of the NCM and SDB that had been made within the time period reported here:

| IDef | Users Data-Base | Delivery by TEC | TEC ref. | Comments |
|------|-----------------|-----------------|----------|----------|
| | | | | |

Table 6: IASI Data Bases for the users

For information, Table 7 shows the delivery applicable at the beginning of the period:

| IDef | Users Data-Base | Delivery by TEC | TEC ref. | Comments |
|------|---|-----------------|-----------|--|
| 2 | IASI_NCM_xx_M01_20130522081244Z_20130522081244Z_20130522081245Z_IASST_SPECTRESPOT | 22/05/13 | CVA_COV_2 | Update of NCM |
| 12 | IASI_SDB_xx_M01_20130923150000Z_20130923150000Z_20130923132439Z_IAST_IASISPECDB | 25/09/13 | R_33 | User database associated to ODB IDefSDB 12 |

Table 7: previous IASI Data Bases

3.5 ON GROUND HW/SW EVOLUTION

Table 8 presents the updates of PPF L1 software within the time period reported here:

| IASI L1 PPF software version | Delivery by TEC | Date introduced on GS1 | Comments |
|------------------------------|-----------------|---|-----------------|
| 7.4 | 13/10/2015 | 25/01/2017 for sensing time 12:26 Orbit 22601 | AIX 7.1 upgrade |

Table 8: IASI L1 PPF Configuration on the Operational EPS Ground Segment

For information, Table 9 shows the software version applicable at the beginning of the period:

| IASI L1 PPF software version | Delivery by TEC | Date introduced on GS1 | Comments |
|------------------------------|-----------------|--|-------------------|
| 7.3 | 08/2015 | 29/09/2015 for sensing time 12:47 ^{UTC} Orbit 15725 | CSQ impact on IIS |

Table 9: Previous IASI L1 PPF

| | | |
|---|---|---|
|  |  | Doc n°: IA-RP-2000-4332-CNE Issue: 1.0 Date: 2017-07-25 Sheet: 13 Of: 60 |
|---|---|---|

3.6 DECONTAMINATION

Table 10 presents decontaminations that have been made or requested within the time period reported here:

| Last due date | Date of decontamination | Description |
|---------------|-------------------------|-------------|
| | | |

Table 10: Decontamination TEC Requests

For information, Table 11 shows the previous decontamination:

| Last due date | Date of decontamination | Description |
|---------------|-------------------------|----------------------|
| End of 2015 | 25-30 November 2015 | Decontamination 200K |

Table 11: Previous decontamination

3.7 INSTRUMENT

3.7.1 External events

This category is for those activities/events that are external to IASI but still have an impact. It is broken down into classes of *PL-SOL* and *OOP* manoeuvre.

3.7.1.1 Manoeuvres

| Date | Type ^(*) | Description | IP flag | OoP mission Outage |
|------------|---------------------|--|---------|--------------------|
| 29/12/2016 | IP | IP manoeuvre #25 (orbit 22223) (collision avoidance) | | |
| 01/02/2017 | IP | IP manoeuvre #26 (orbit 22700) | | |

Table 12: Overview of METOP manoeuvres in the reporting period

(^{*}): IP for In-Plane manoeuvres (IASI stays in NOP) and OoP for Out of plane manoeuvres (IASI is put in Heater 2)

3.7.1.2 PL-SOL

Table 13 presents the PL-SOL events that have occurred within the time period reported here:

| Dates | Orbits | Description |
|-------|--------|-------------|
| | | |

Table 13: PL-SOL

3.7.2 Operation leading to mission outage

This chapter presents the intervention on IASI needing routine interruption that have occurred within the time period reported here.

| Dates | Orbits | type | IASI mode | Description |
|-------|--------|------|-----------|-------------|
| | | | | |

Table 14: Scheduled interruptions

| | | |
|---|---|---|
|  |  | Doc n°: IA-RP-2000-4332-CNE Issue: 1.0 Date: 2017-07-25 Sheet: 14 Of: 60 |
|---|---|---|

3.7.3 Anomaly leading to mission outage

Table 15 and Table 16 present the major and minor anomalies internal to IASI that have occurred within the time period reported here.

Note that, in this section minor anomalies are all identified and without any impact on the mission, and major anomalies only affect IASI instrument, and no other sub-systems of the spacecraft.

| Dates | Orbits | Anomaly type (*) | IASI mode | Description |
|------------|--------|----------------------------|-----------|--------------------------------|
| 15/12/2016 | 22016 | NormOp → NormOp transition | | NOp transition → auto-recovery |

Table 15: Major anomalies

(*): SEU (LAS, CCM or DPS) anomalies or SET anomalies

| Day | Orbits | error n° | Severity | Anomaly type | LN | SN | Description |
|-----|--------|----------|----------|--------------|----|----|-------------|
| | | | | | | | |

Table 16: Minor anomalies

| | | |
|---|---|---|
|  |  | Doc n°: IA-RP-2000-4332-CNE Issue: 1.0 Date: 2017-07-25 Sheet: 15 Of: 60 |
|---|---|---|

4 **PERFORMANCE MONITORING**

4.1 ***PERFORMANCE MONITORING***

In order to ensure that the IASI system is permanently running in good conditions, the CNES (IASI TEC) and EUMETSAT (CGS) are monitoring products at various temporal levels : at line, PDUs and DUMP (full orbit).

The on-board and ground processing performance algorithms issue more than one hundred quality indicators, called flags and simple parameters. Those are alarms for any bad functioning or local performance degradation.

According to the results, the TEC is also in charge of delivering new on-board or ground parameters to EUMETSAT when it is necessary. EUMETSAT is then in charge of uploading them on-board or as an input of the level 1 processing chain. During the whole instrument life, these parameter adjustments are necessary in order to take into account instrument evolution in the processing and finally to maintain a good data quality.

The Table 17 is the colour code used for the status report.

| Status Colour | Meaning |
|---------------|-----------------------------|
| GREEN | $\geq 95\%$ of good spectra |
| YELLOW | < 95% of good spectra |
| RED | Production interrupted |
| BLANK | No Status Reported |

Table 17: Functional status legend

| | | |
|---|---|---|
|  |  | Doc n°: IA-RP-2000-4332-CNE Issue: 1.0 Date: 2017-07-25 Sheet: 16 Of: 60 |
|---|---|---|

4.2 PERFORMANCE SYNOPSIS

Table 18 provides a synthetic view of all the indicators evaluated for L0/L1 data and their current status.

| Section | Component | Description | Status | Comments |
|---------------------|-----------|---|--------|----------------------|
| 4.3 | L0 | Level-0 Data Quality <ul style="list-style-type: none"> Overall quality Main flag and quality indicator parameters - Spikes monitoring - ZPD monitoring - Overflows/Underflows monitoring - Reduced Spectra monitoring Second level flag and quality indicators | GREEN | On-board processing |
| 4.4 | L1 | Level-1 Data Quality <ul style="list-style-type: none"> Overall quality Main flag and quality indicator parameters | GREEN | On ground processing |
| 4.5 | L1 | Sounder radiometric performances <ul style="list-style-type: none"> Radiometric noise Radiometric calibration Acquisition chain delay Optical transmission <ul style="list-style-type: none"> - Ice - Prediction of decontamination date Interferometric contrast Interferogram Baseline Detection chain | GREEN | |
| 4.6 | L1 | Sounder spectral performances <ul style="list-style-type: none"> Dimensional stability <ul style="list-style-type: none"> - Position of axis - Cube Corner constant offset - Cube Corner velocity - Optical bench temperature Spectral calibration | GREEN | |
| 4.7 | L1 | Geometric performances <ul style="list-style-type: none"> Sounder/IIS co-registration IIS/AVHRR co registration | GREEN | |
| 4.8 | L1 | IASI-B inter-calibration <ul style="list-style-type: none"> IASI-B inter-calibration with IASI-A IASI-B inter-calibration with CRIS IASI-B inter-calibration with AIRS | GREEN | |
| 4.9 | L1 | IIS radiometric performances | GREEN | |

Table 18: IASI product components functional status

| | | |
|---|---|---|
|  |  | Doc n°: IA-RP-2000-4332-CNE Issue: 1.0 Date: 2017-07-25 Sheet: 17 Of: 60 |
|---|---|---|

4.3 LEVEL 0 DATA QUALITY (L0)

4.3.1 Overall quality

The IASI L0 data quality (orbit average) through IASI engineering products is shown in Figure 1.

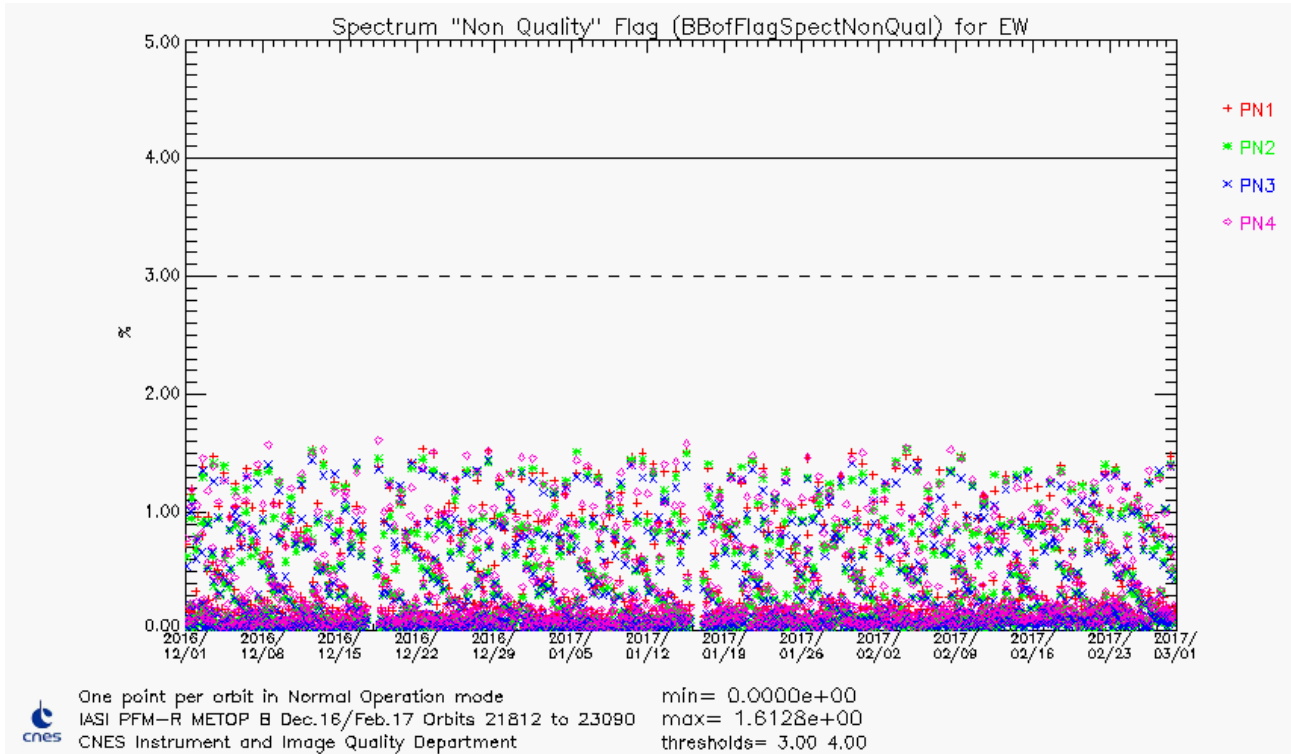


Figure 1 : IASI L0 data quality orbit average (per pixel and CCD)

The geographical distribution of the overall L0 (board) quality flag for the 4 pixels is shown in Figure 2.

| | | |
|---|---|-----------------------------|
|  |  | Doc n°: IA-RP-2000-4332-CNE |
| | | Issue: 1.0 |
| | | Date: 2017-07-25 |
| | | Sheet: 18 Of: 60 |

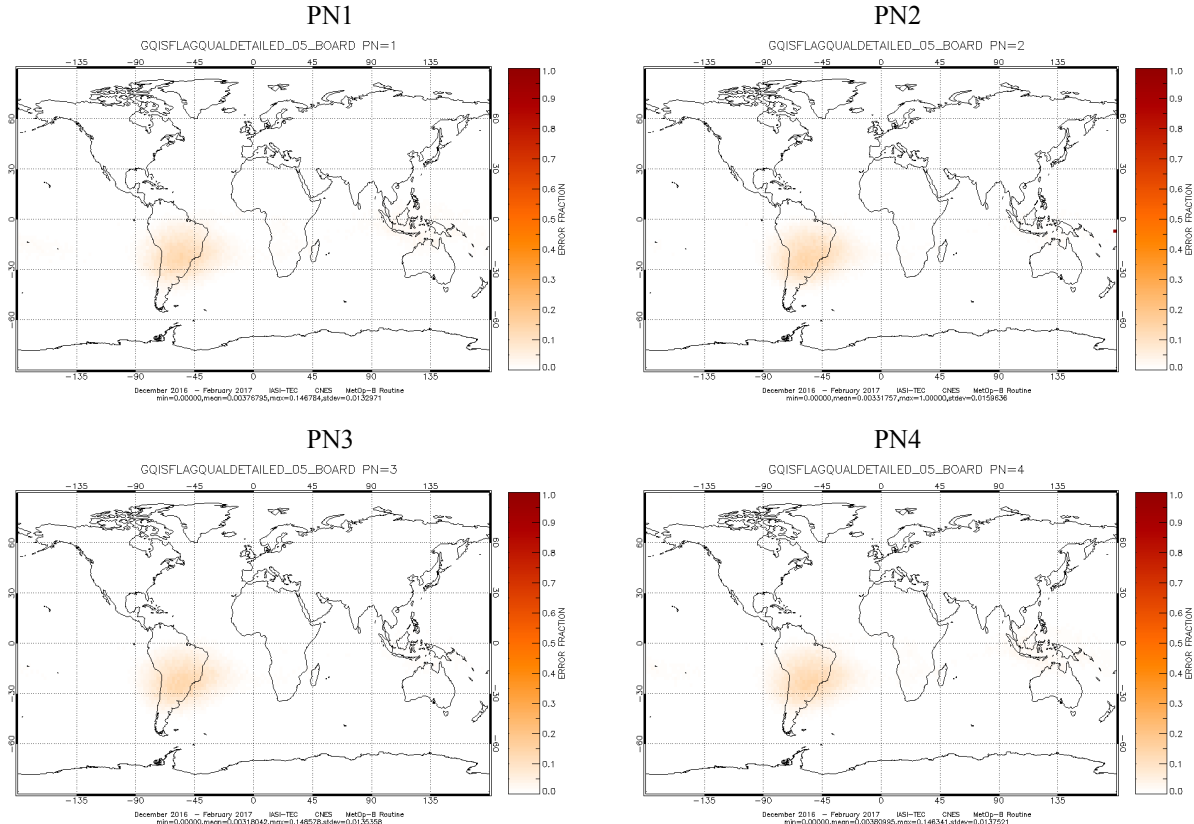


Figure 2 : IASI L0 data quality spatial distribution (per pixel)

The IASI L0 quality and on-board processing are nominal.

| | | |
|---|---|---|
|  |  | Doc n°: IA-RP-2000-4332-CNE Issue: 1.0 Date: 2017-07-25 Sheet: 19 Of: 60 |
|---|---|---|

4.3.2 Main flag and quality indicator parameters

The main contributors to the rejected spectra by on-board processing are: spikes (proton interaction on detectors), failure of NZPD algorithm determination and over/underflows (measured data exceeding on-board coding tables capacity). They are analysed in details hereafter.

4.3.2.1 Spikes monitoring

Spikes occur when a proton hits a detector. This very high energetic particle disrupts the measure of the interferogram and then corrupts the spectrum.

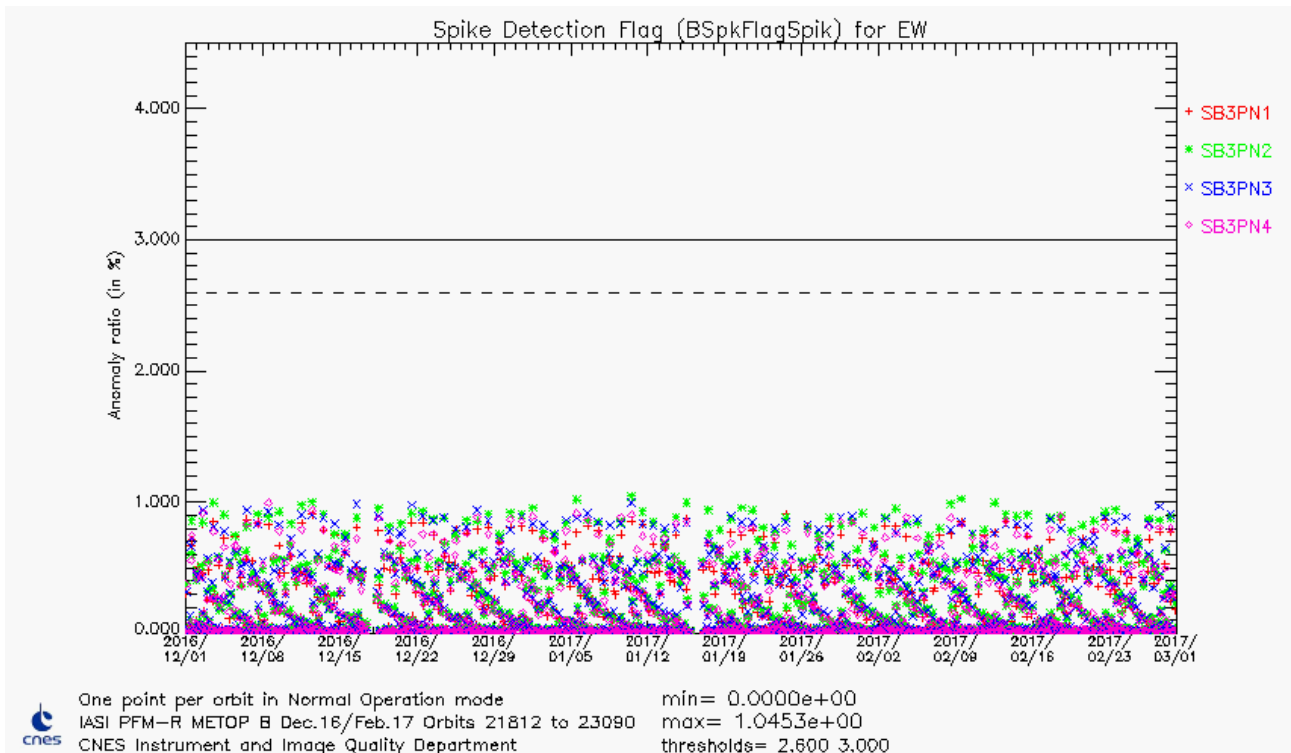


Figure 3 : Temporal evolution of spikes anomaly ratio in % for all pixels (orbit average)

An example of the geographical distribution of spikes occurrences on band 3 for the 4 pixels is shown in Figure 4.

| | | |
|---|---|-----------------------------|
|  |  | Doc n°: IA-RP-2000-4332-CNE |
| | | Issue: 1.0 |
| | | Date: 2017-07-25 |
| | | Sheet: 20 Of: 60 |

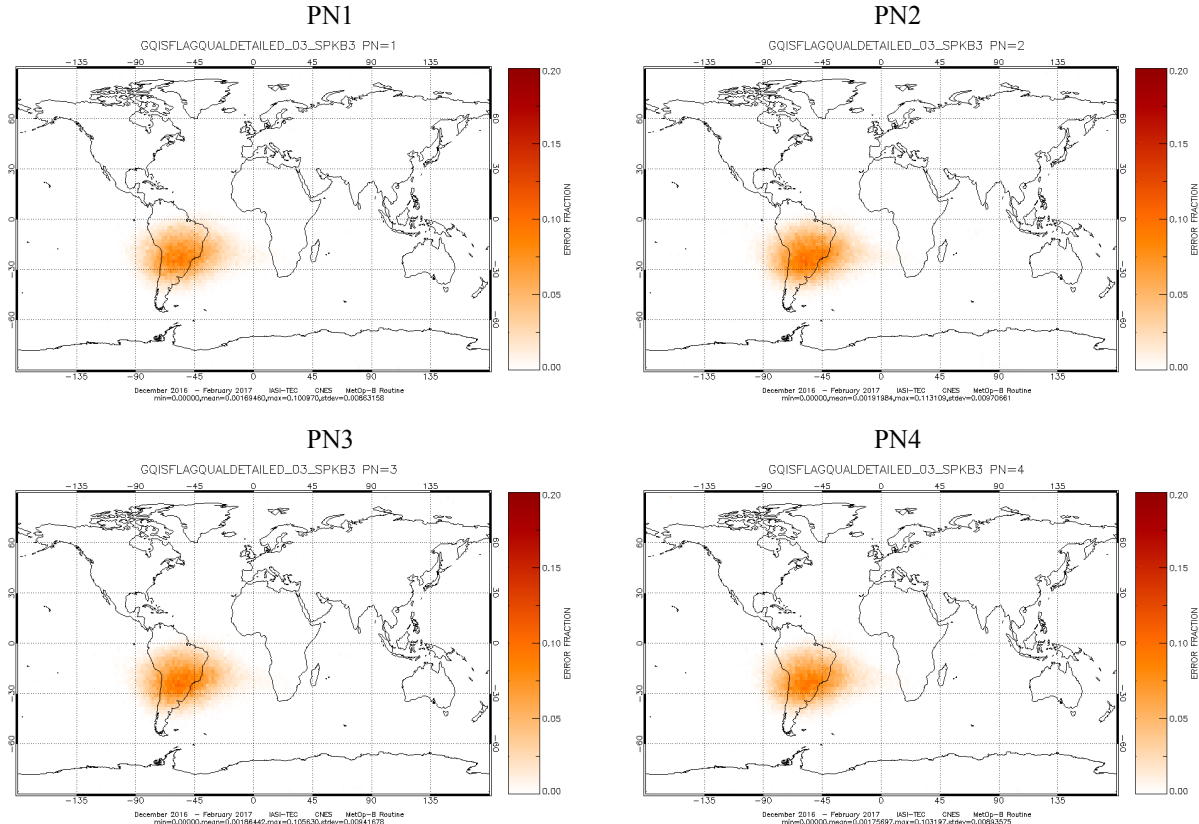


Figure 4 : Geographical distribution of spikes occurrences in % for band 3 and all pixels

Spikes are mainly located in the regions of Earth where the magnetic field doesn't protect the satellite from the energetic particles: the poles and the SAA (South Atlantic anomaly).

Spike anomaly ratio is nominal for the reported period.

| | | |
|---|---|---|
|  |  | Doc n°: IA-RP-2000-4332-CNE Issue: 1.0 Date: 2017-07-25 Sheet: 21 Of: 60 |
|---|---|---|

4.3.2.2 ZPD monitoring

The ZPD (“Zero Path Difference”) is the position of the central fringe of the interferogram. The NZPD is the number of the sample detected as the ZPD. On IASI, it is determined by a software. This is a special feature of IASI in comparison to other instruments for which NZPD determination is done by hardware.

NZPD variations are governed by two phenomena:

1. ASE fluctuations which have the same effect on each pixel and can produce NZPD variation of 30-40 samples over month. This is the first order phenomena.
2. Mechanical deformation of the interferometer or evolution of detection chain delays. These phenomena affect the 4 pixels in different way. However this phenomenon has a second order effect in comparison to the first one.

We monitor both NZPD determination quality flag and interpixel homogeneity. We expect stability.

BZPDFlagNZPDNonQualEW: Temporal evolution of NZPD determination quality flag for earth view

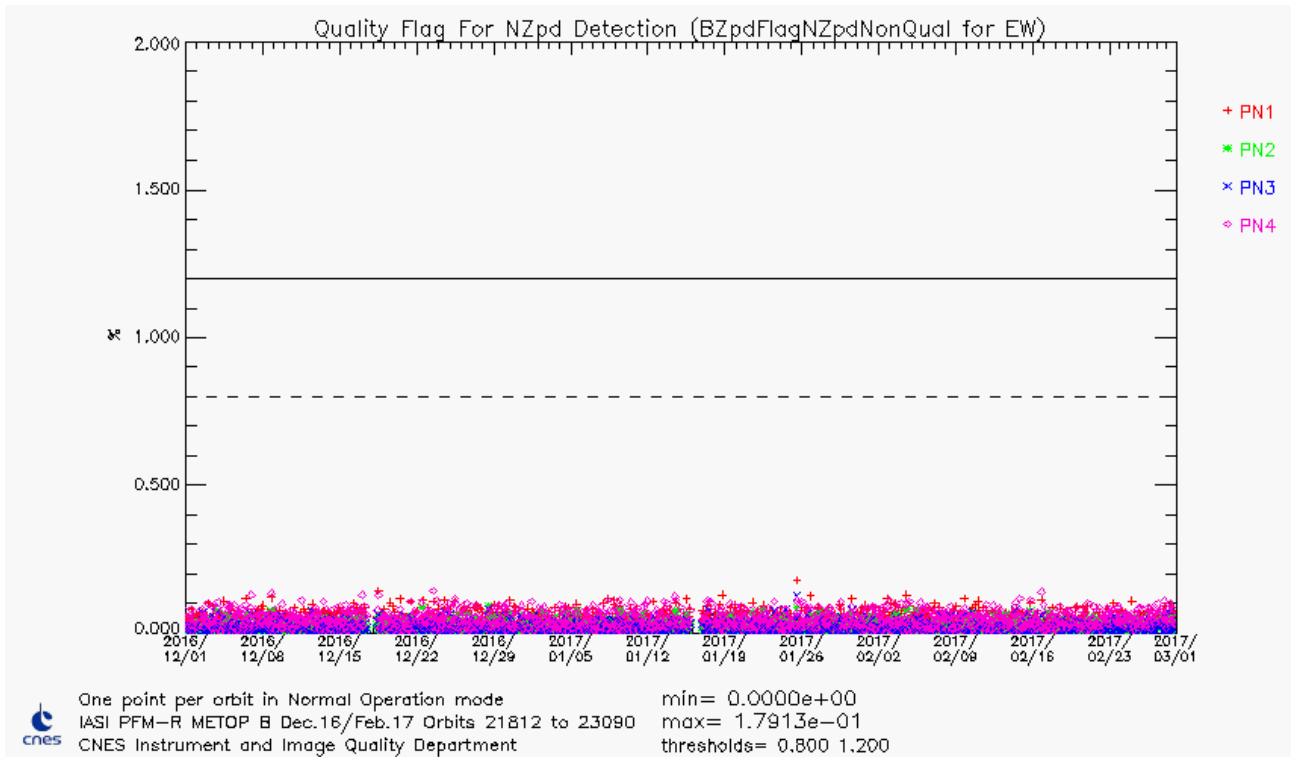


Figure 5 : Temporal evolution of NZPD determination anomaly ratio in % for all pixels (orbit average)

NZPD determination anomaly ratio is nominal for the reported period.

The geographical distribution of the NZPD determination quality flag for the 4 pixels is shown in Figure 6.

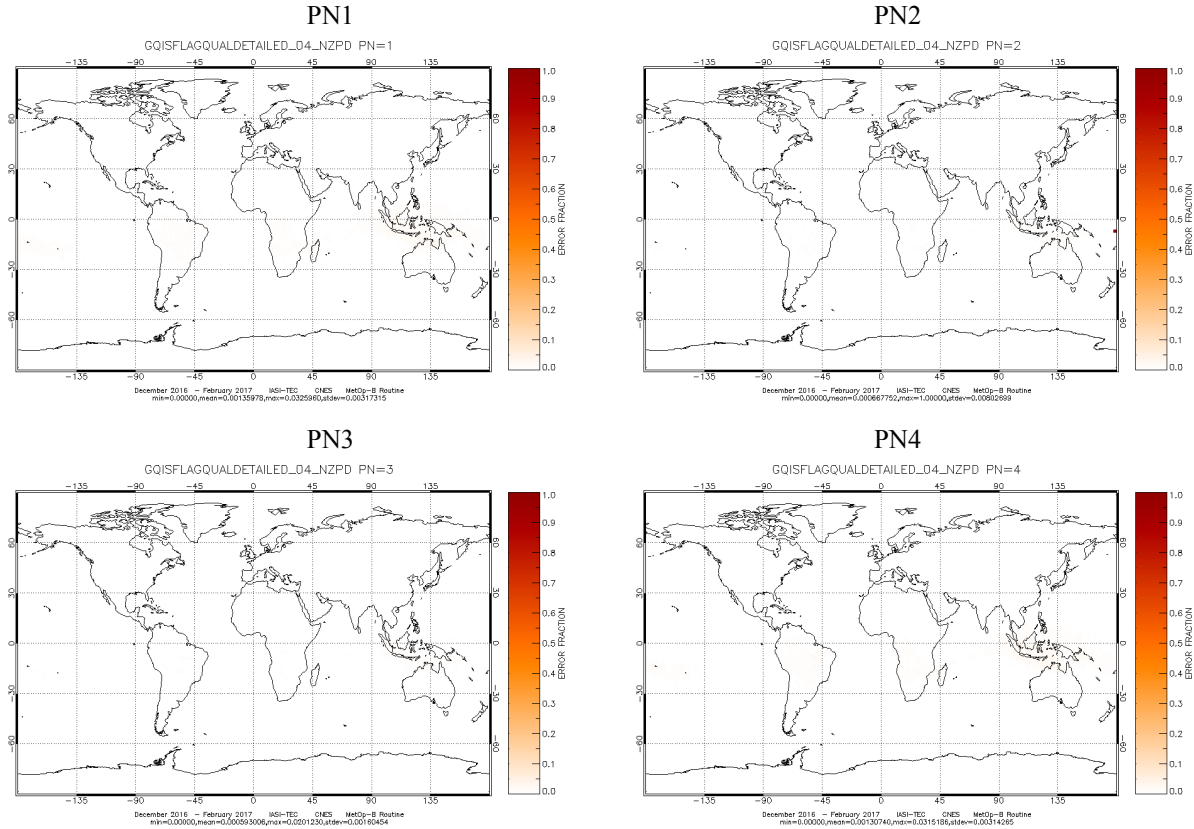


Figure 6 : IASI NZPD determination quality flag spatial distribution (per pixel)

The NZPD determination fails over some clouds that have a temperature that induces no energy in the central fringe of the interferogram.

| | | |
|---|---|---|
|  |  | Doc n°: IA-RP-2000-4332-CNE Issue: 1.0 Date: 2017-07-25 Sheet: 23 Of: 60 |
|---|---|---|

NZPD inter-pixel homogeneity monitoring

This monitoring is necessary in order to follow potential deformation of the interferometer or evolution of detection chain delay.

The NZPD inter-pixel homogeneity is nominal over the reported period. Consequently, these parameters are perfectly stable and in-line with the specification.

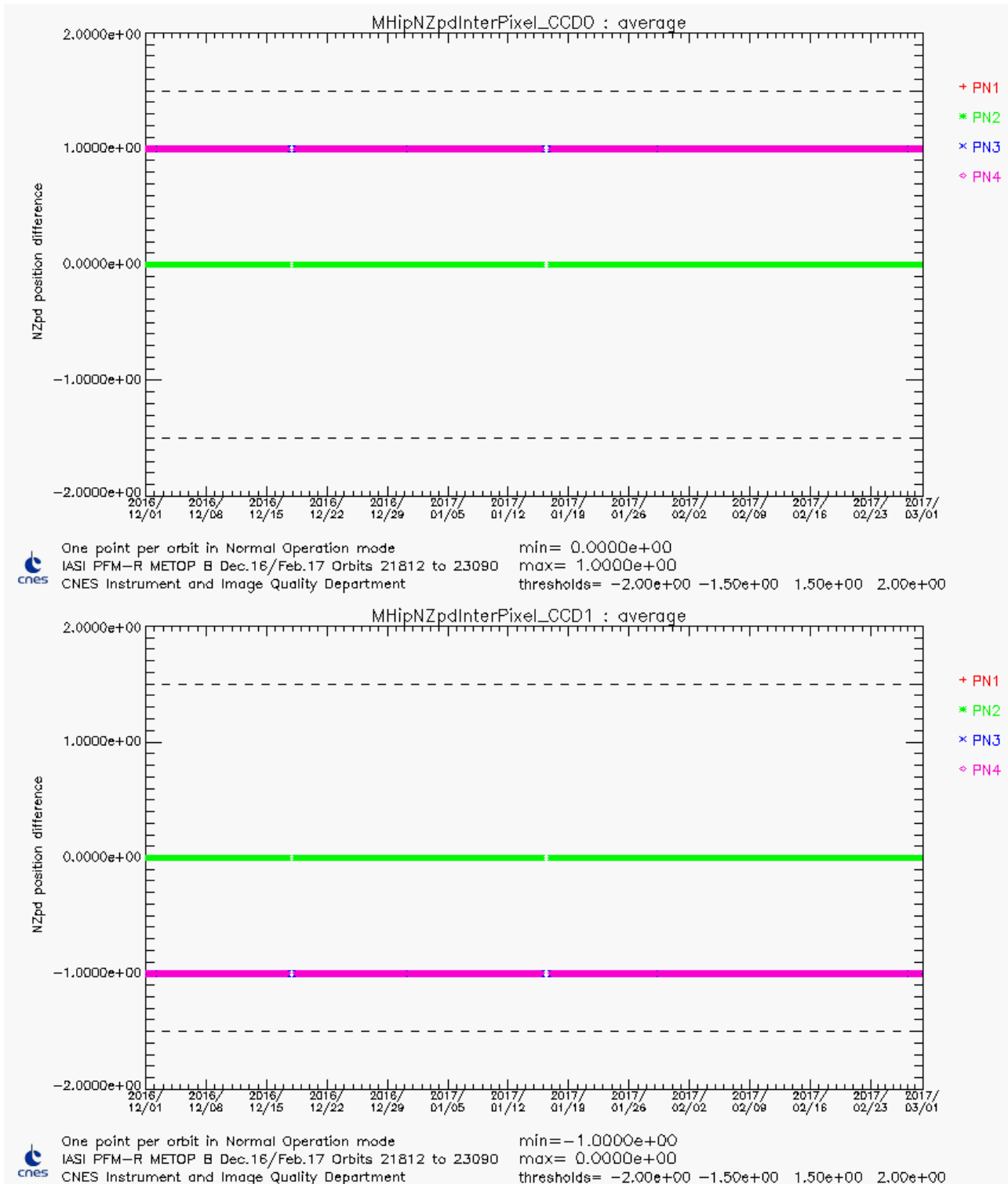


Figure 7 : NZPD inter-pixel for all pixels and CCD calculated with respect to pixel 1 (orbit average)

| | | |
|---|---|-----------------------------|
|  |  | Doc n°: IA-RP-2000-4332-CNE |
| | | Issue: 1.0 |
| | | Date: 2017-07-25 |
| | | Sheet: 24 Of: 60 |

4.3.2.3 Overflows / Underflows monitoring

The total number of bits available for a spectrum to be transmitted to the ground is limited. For that reason, we have defined coding tables to encode each measured spectrum. These tables have been designed by using “extreme spectrum” corresponding to known drastic atmospheric conditions. The coding step is also set to not introduce additional noise into the spectrum. However for very extreme atmospheric conditions (sunglint in B3, very high stratospheric temperature...) a measurement can exceed on-board coding tables’ capacity and causes an over/underflow.

Over/underflows occurrences are monitored and stability is expected. As long as they remain to low levels, the coding table is not changed. Note that changing the coding tables requires compromises. Indeed, increasing the encoding capacity can be achieved by two different ways. A first solution consists in an increase of the coding step without changing the number of bits. However, that leads to an increase of the digitalization noise. Then, a second solution consists in keeping the coding step constant while increasing the number of bits available for a particular band. But, the total amount of bits available for the entire spectrum is limited and constant. So, that requires to decrease the encoding capacity in another spectral band.

Time series of Overflows and Underflows (orbit average) are shown in following figure for all pixels.

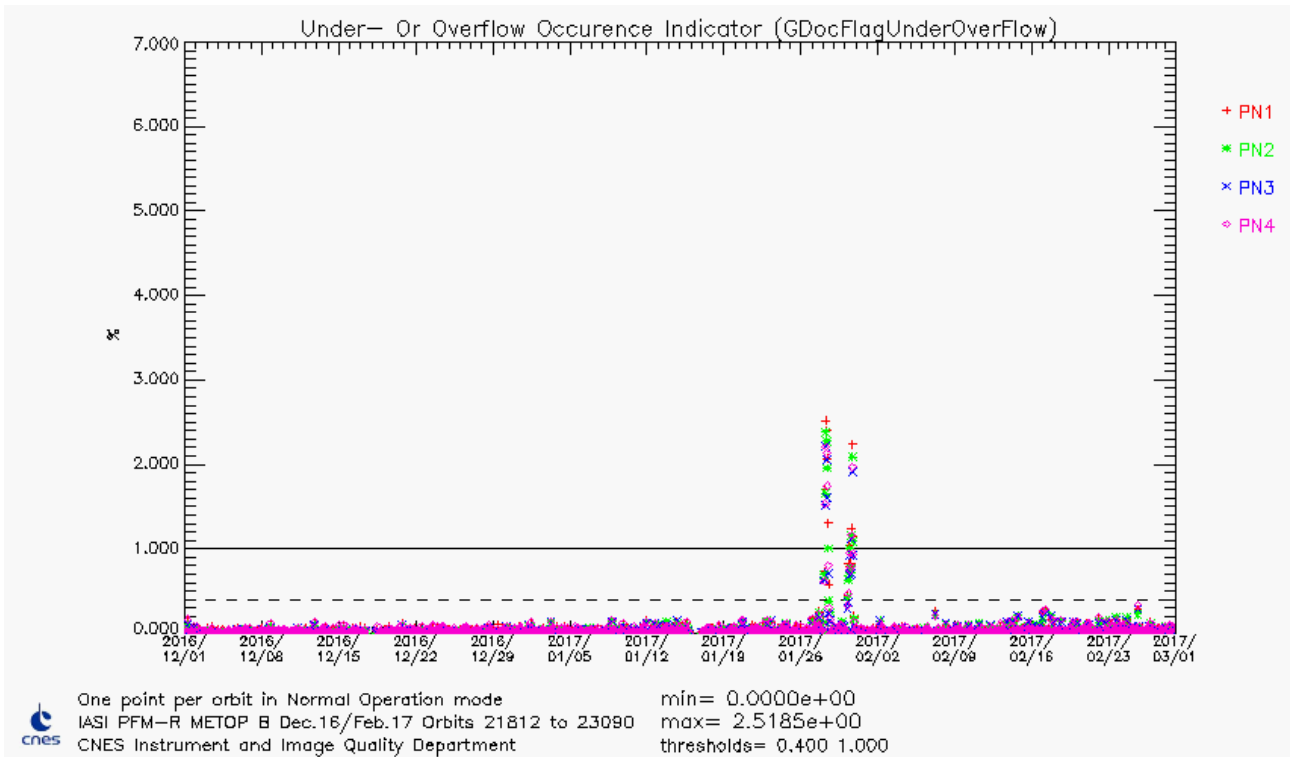


Figure 8 : IASI L0 over/under-flows orbit average of all pixels

Over/underflows ratio is nominal for the reported period.

Note: the peak observed on the figure is due to high stratospheric temperature. This phenomenon is related to the polar vortex collapse of the winter hemisphere. The consequence for IASI system is that the on-board coding tables are not able to encode this type of exceptional event around 2350-2400 cm⁻¹ (CO₂ band).

The geographical distribution of the Overflows and Underflows for the 4 pixels shown in Figure 9 clearly indicates the polar vortex collapse.

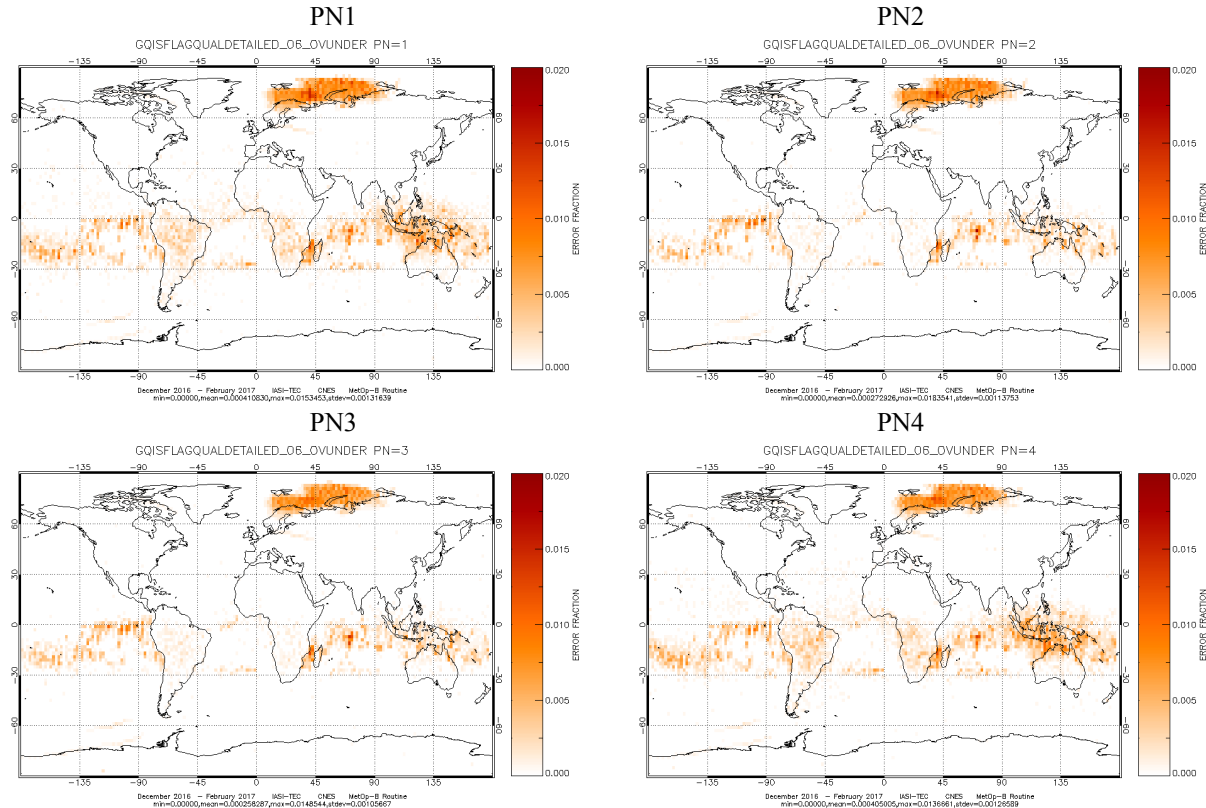


Figure 9 : IASI Overflows and Underflows spatial distribution (per pixel)

| | | |
|---|---|---|
|  |  | Doc n°: IA-RP-2000-4332-CNE Issue: 1.0 Date: 2017-07-25 Sheet: 26 Of: 60 |
|---|---|---|

4.3.2.4 Reduced Spectra monitoring

On-board Reduced Spectra is one of the most important parameter to monitor. It ensures that on-board spectra still have a good radiometric calibration when on-board configuration reduced spectra are reloaded. This is the case, for instance, after an instrument mode change.

Reduced spectra are slightly evolving with respect to potential deformation of the interferometer (optical bench).

In order to prevent from a large difference between current and on-board configuration reduced spectra, we apply the DPS processing on the verification interferograms using the reduced spectra from the on-board configuration (TOP) instead of the filtered reduced spectra computed on-board with the current calibration views. These reduced spectra from the on-board configuration are used as initialisation each time there is mode change. If they are too far from the reality, no spectra can be computed on-board after a mode change. We monitor the evolution of ZPD determination quality index for calibration views (BZpdNzpdQualIndexBB and CS) obtained by this DPS processing at TEC, results of this monitoring are given hereafter.

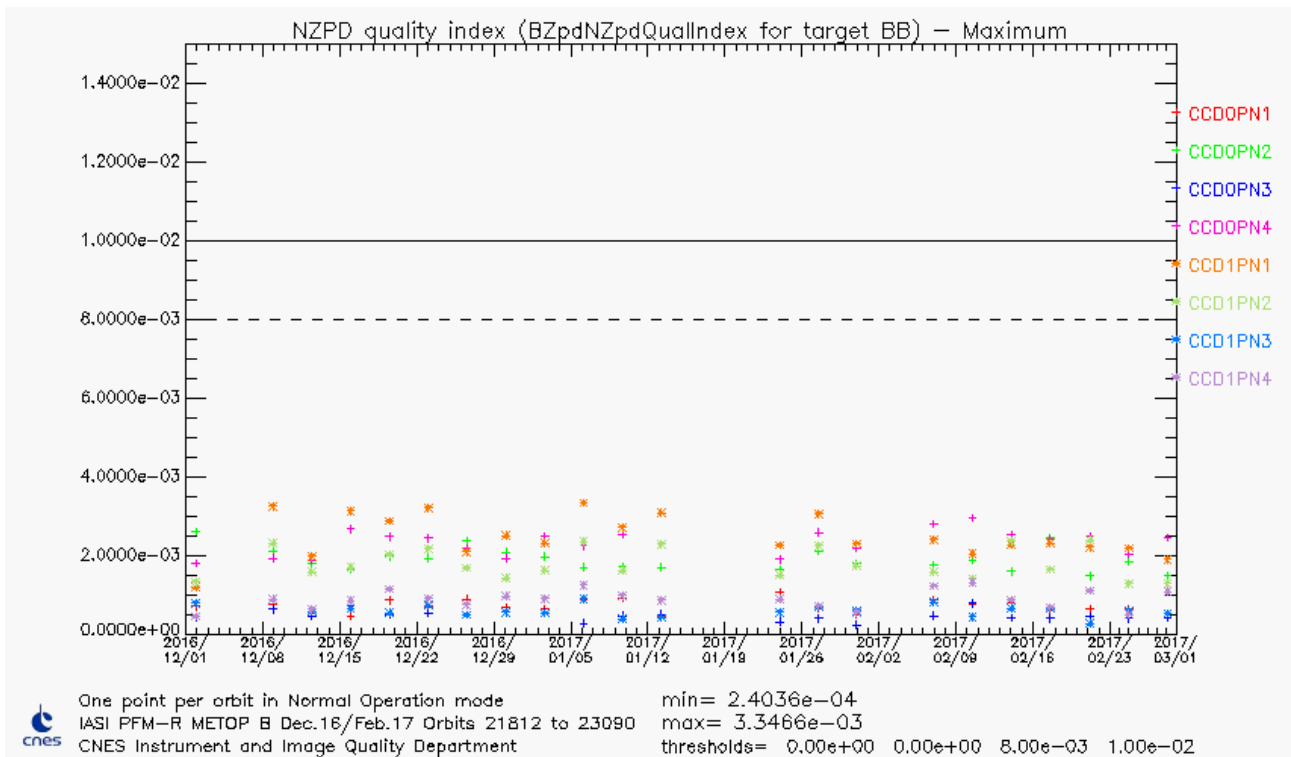


Figure 10 : Max of NZPD quality index for all pixels and CCD - BB

| | | |
|---|---|---|
|  |  | Doc n°: IA-RP-2000-4332-CNE Issue: 1.0 Date: 2017-07-25 Sheet: 27 Of: 60 |
|---|---|---|

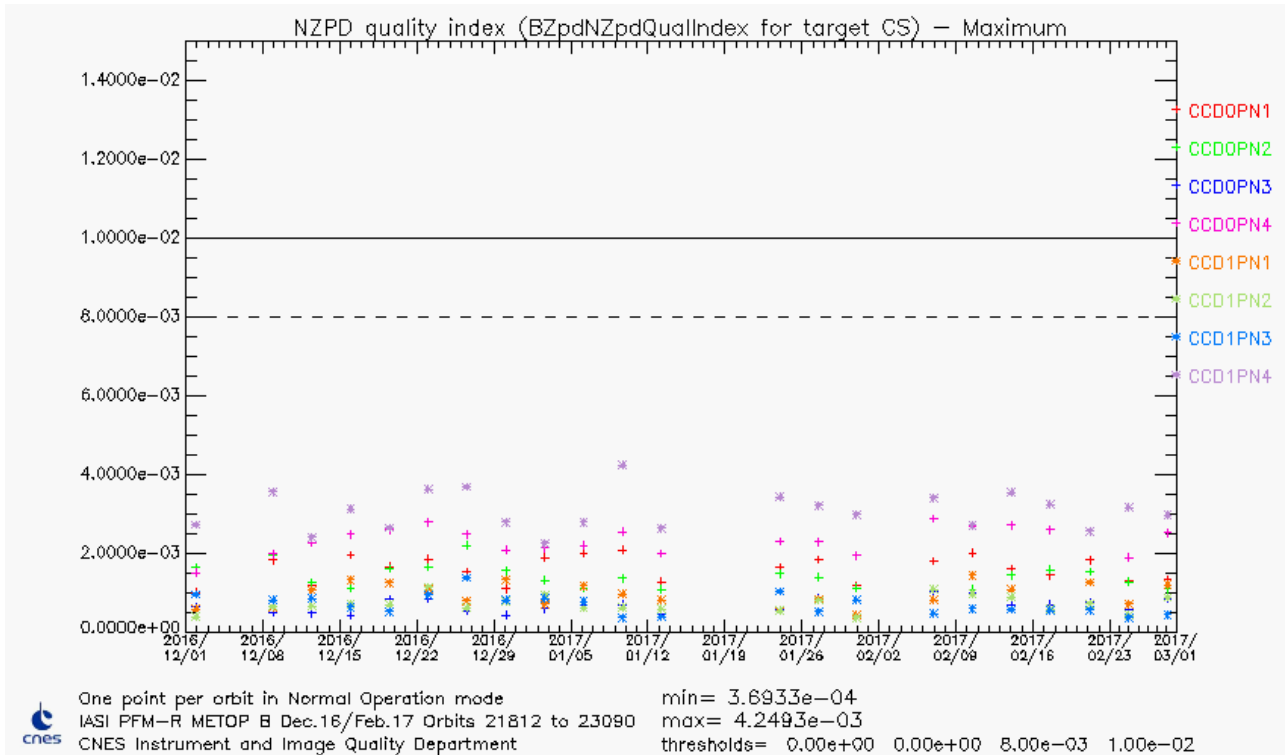


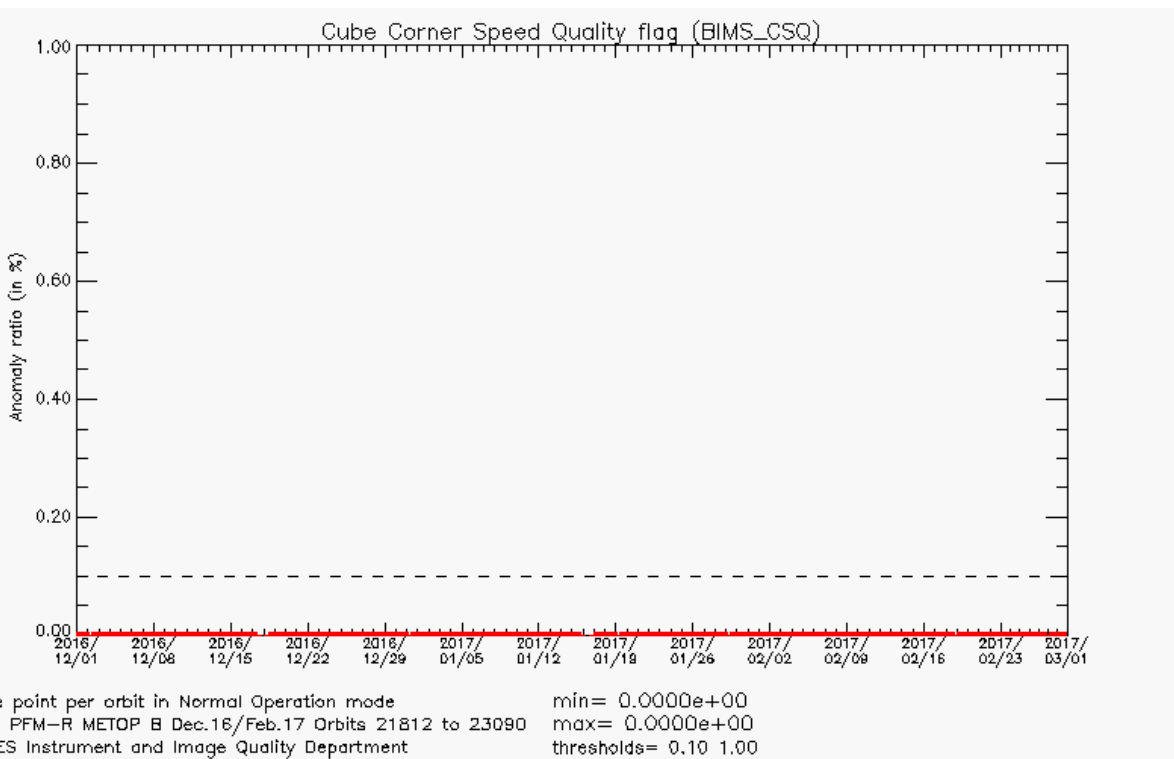
Figure 11 : Max of NZPD quality index for all pixels and CCD - CS

As soon as BZPDNZPDQualIndexBB and CS remain below 0.02 on-board reduced spectra are robust to an instrument mode change.

The reduced spectra quality is well within specification since the last update of the on-board reduced spectra performed in February 2015.

4.3.2.5 Cube corner Speed Quality (CSQ) monitoring

From verification products (BB & CS):



| | | |
|---|---|---|
|  |  | Doc n°: IA-RP-2000-4332-CNE Issue: 1.0 Date: 2017-07-25 Sheet: 28 Of: 60 |
|---|---|---|

From engineering products (EW):

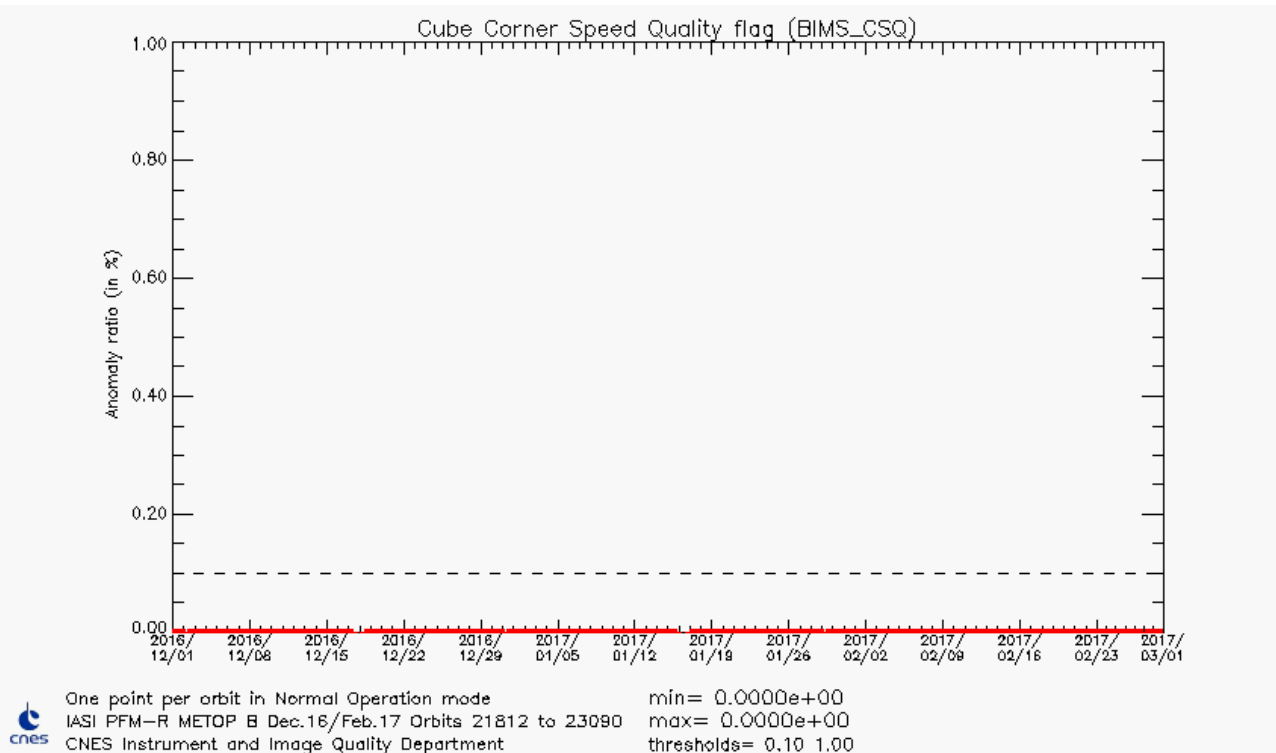


Figure 12 : Number of CSQ

4.3.3 Second level flags and quality indicators

All second level flags and indicators are stable and nominal.

4.3.4 Conclusion

L0 Flag and quality indicators are stable.

| | | |
|---|---|---|
|  |  | Doc n°: IA-RP-2000-4332-CNE Issue: 1.0 Date: 2017-07-25 Sheet: 29 Of: 60 |
|---|---|---|

4.4 LEVEL 1 DATA QUALITY (L1)

4.4.1 Overall quality

The IASI overall quality is shown as the orbit averages of the quality indicator for the individual pixels in the next figure.

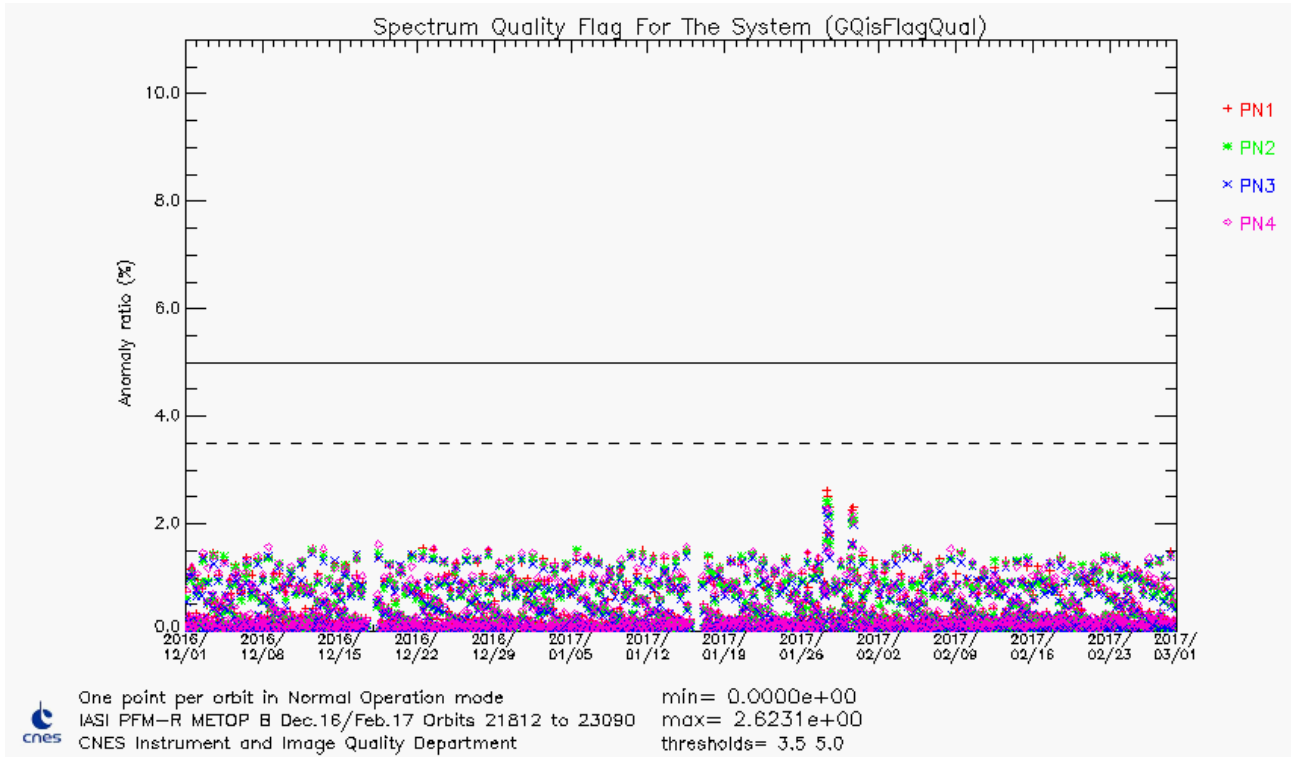


Figure 13 : IASI L1 data quality orbit average (% of bad by PN)

One should note that, over the period covered by the present document, the averaged data rejection ratio is less than 1%. We clearly see that data quality is better on the bands B1 and B2 in comparison to band B3 (which is the most affected by spikes).

Note that the peaks on End January are related to the overflows event (see §4.3.2.3).

The geographical distribution of the IASI product overall quality for the 4 pixels is shown in Figure 14.

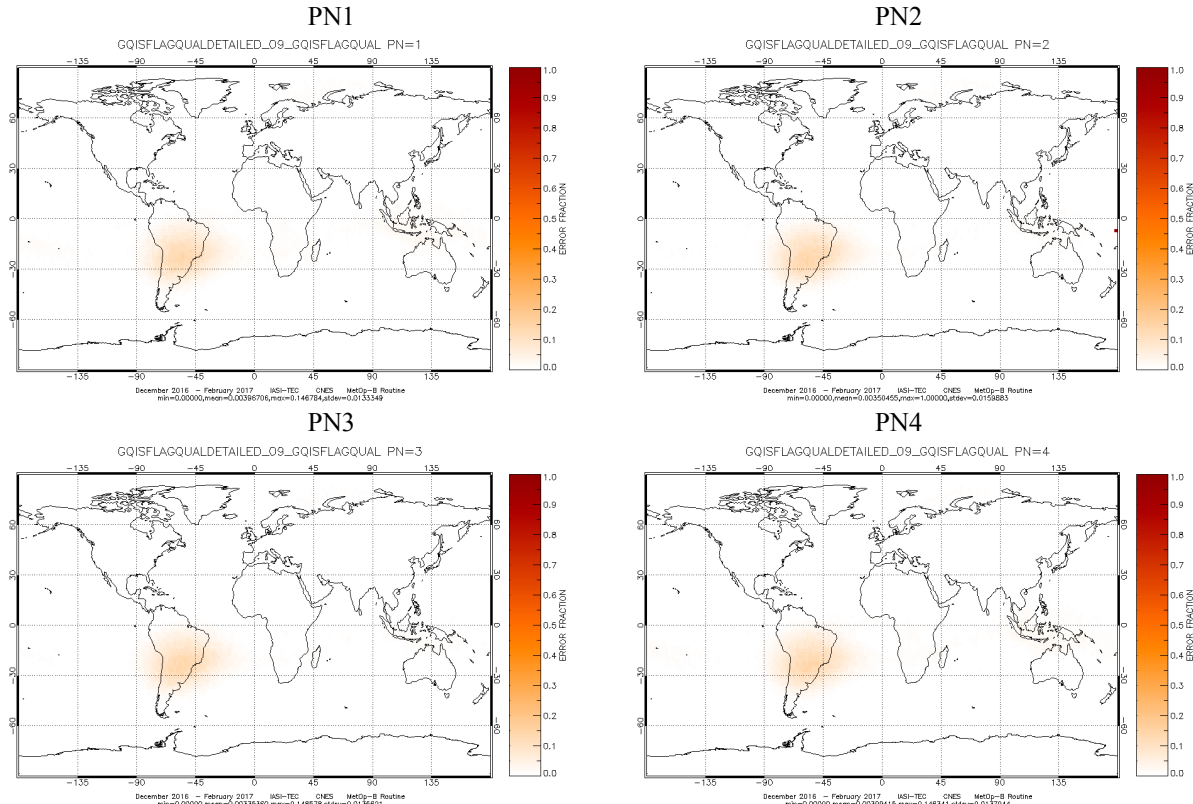


Figure 14 : IASI product overall quality spatial distribution (per pixel)

The main contributors are the spikes (mainly in band 3, which is the band the most sensitive to the spikes).

4.4.2 Main flag and quality indicator parameters

All the quality indexes that follow are general L1 quality indexes of sounder products.

GQisQualIndex – average – is the average general quality index of the sounder products.

GQisQualIndexIIS is the IASI integrated imager (IIS) images quality index.

GQisQualIndexSpect is the spectral quality index of the sounder products.

GQisQualIndexRad is the radiometric quality index of the sounder products.

GqisQualIndexLoc is the ground localisation quality index of the sounder products.

MDptPixQual is a quality index for IASI integrated imager (IIS) that represents a fraction of not dead pixels.

| | | |
|---|---|---|
|  |  | Doc n°: IA-RP-2000-4332-CNE Issue: 1.0 Date: 2017-07-25 Sheet: 31 Of: 60 |
|---|---|---|

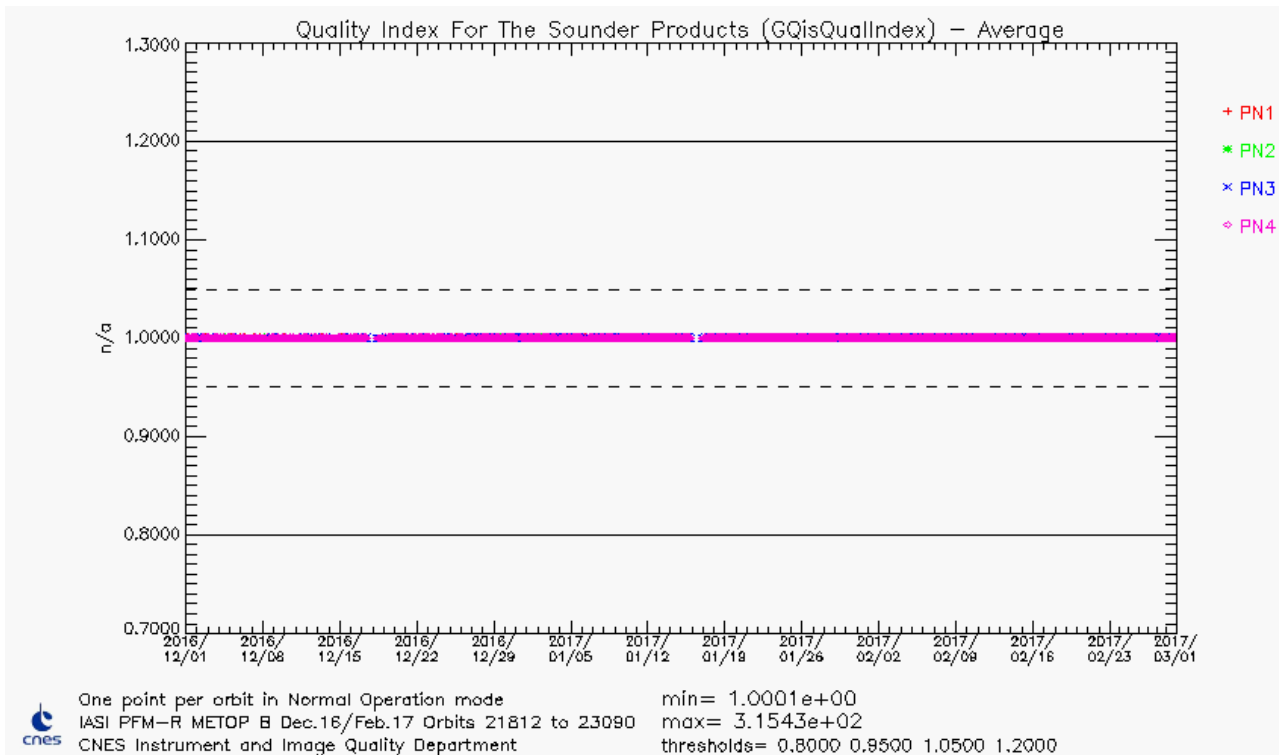


Figure 15 : GQisQualIndex average (L1 data quality index for IASI sounder)

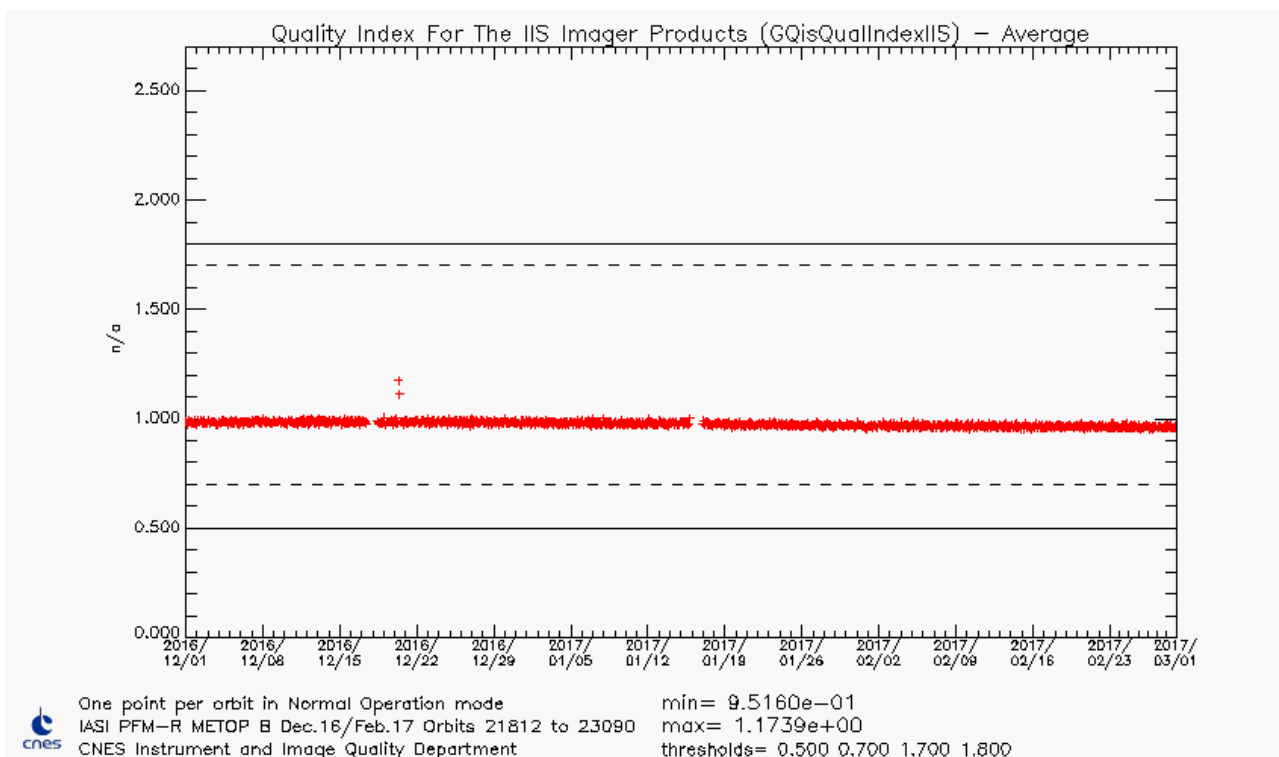


Figure 16 : GQisQualIndexIIS average (L1 data quality index for IASI Integrated Imager)

| | | |
|---|---|---|
|  |  | Doc n°: IA-RP-2000-4332-CNE Issue: 1.0 Date: 2017-07-25 Sheet: 32 Of: 60 |
|---|---|---|

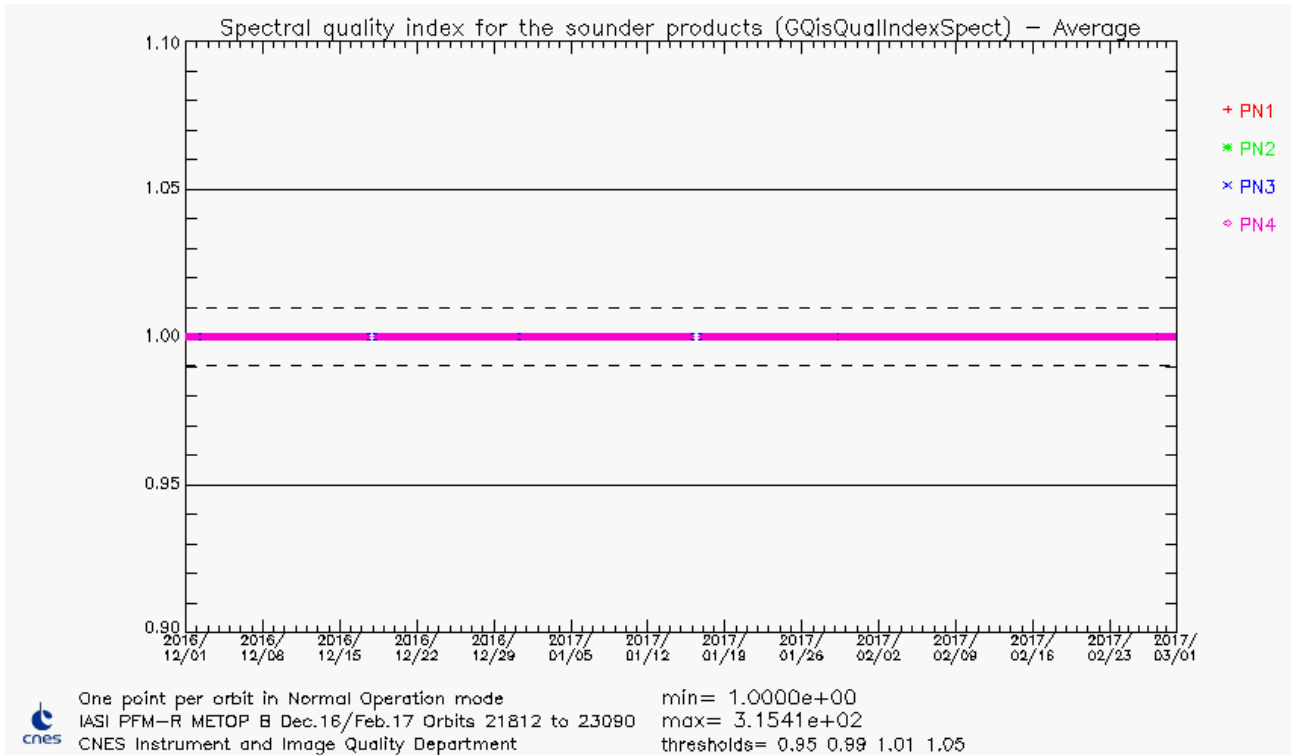


Figure 17 : GQisQualIndexSpect average (L1 data index for spectral calibration quality)

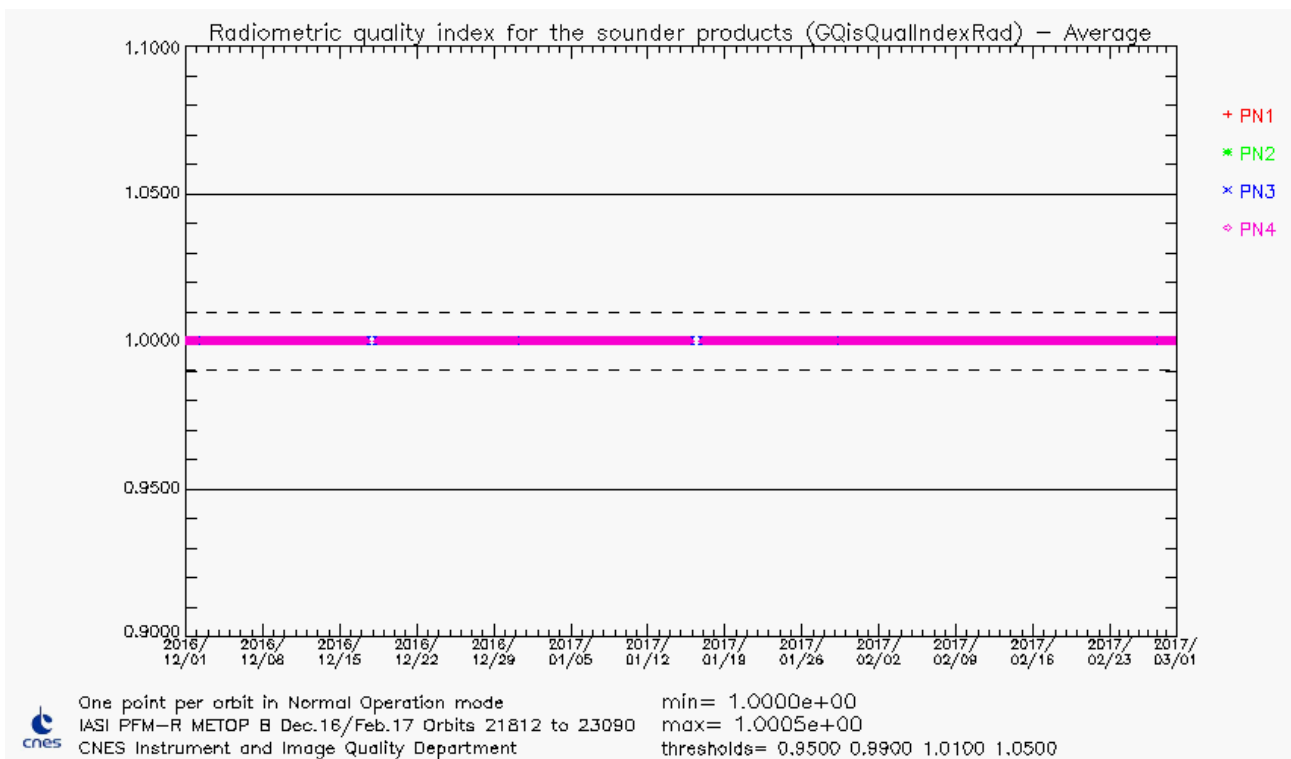


Figure 18 : GQisQualIndexRad average (L1 data index for radiometric calibration quality)

| | | |
|---|---|---|
|  |  | Doc n°: IA-RP-2000-4332-CNE Issue: 1.0 Date: 2017-07-25 Sheet: 33 Of: 60 |
|---|---|---|

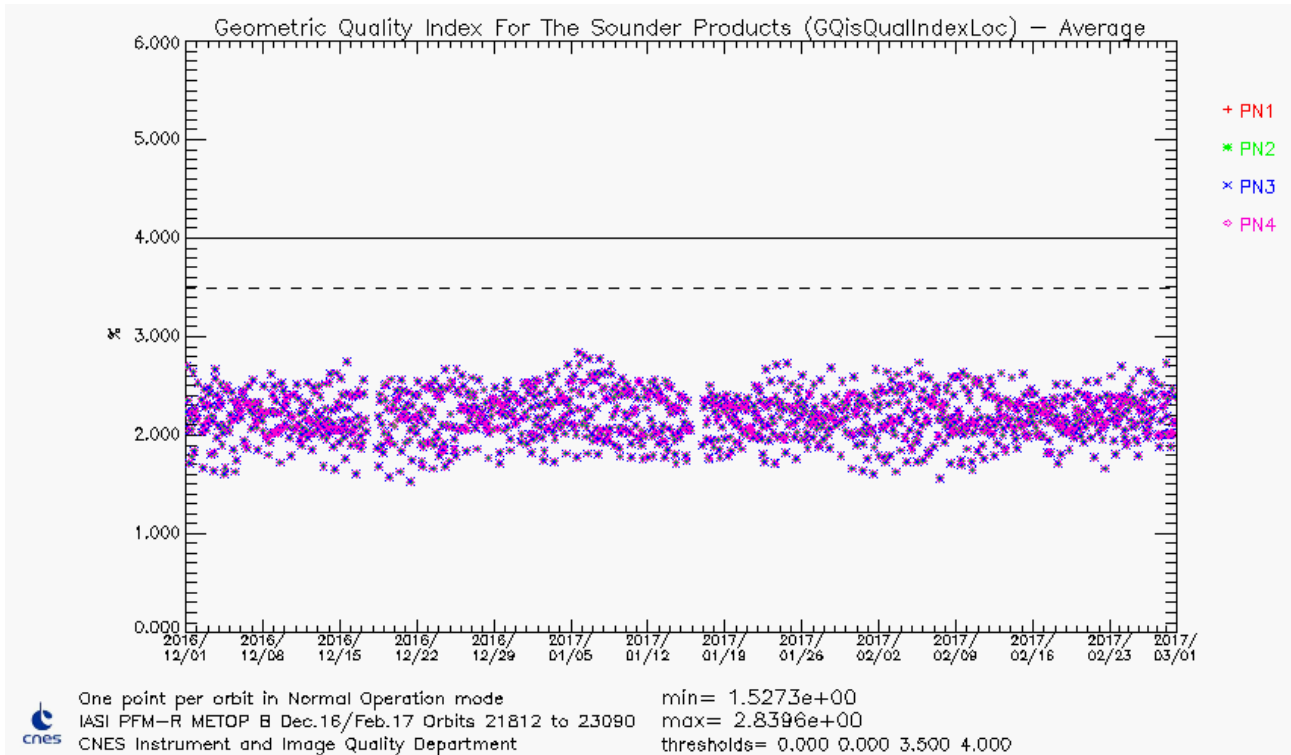


Figure 19 : GQisQualIndexLoc average (L1 data index for ground localisation quality)

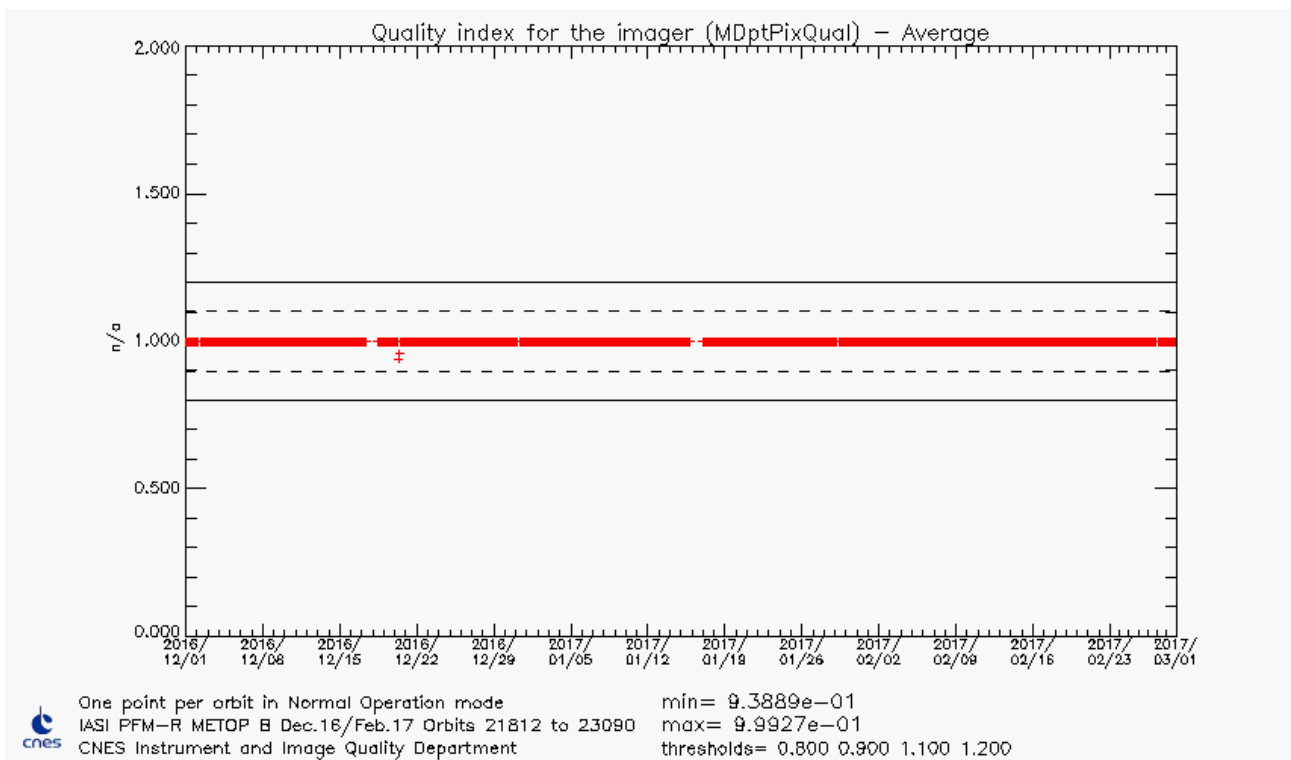


Figure 20 : MDptPixQual average (L1 quality index for IASI integrated imager, fraction of not dead pixels)

4.4.3 Conclusion

L1 Flag and quality indicators are stable and meet the specifications.

4.5 SOUNDER RADIOMETRIC PERFORMANCES

4.5.1 Radiometric Noise

Monitoring the radiometric noise allows to monitor the long term degradation of the instrument as well as to look for punctual anomaly of IASI or other component of METOP.

Monthly L0 noise estimation (CE)

This monthly estimation is performed during routine External Calibration on BB views.

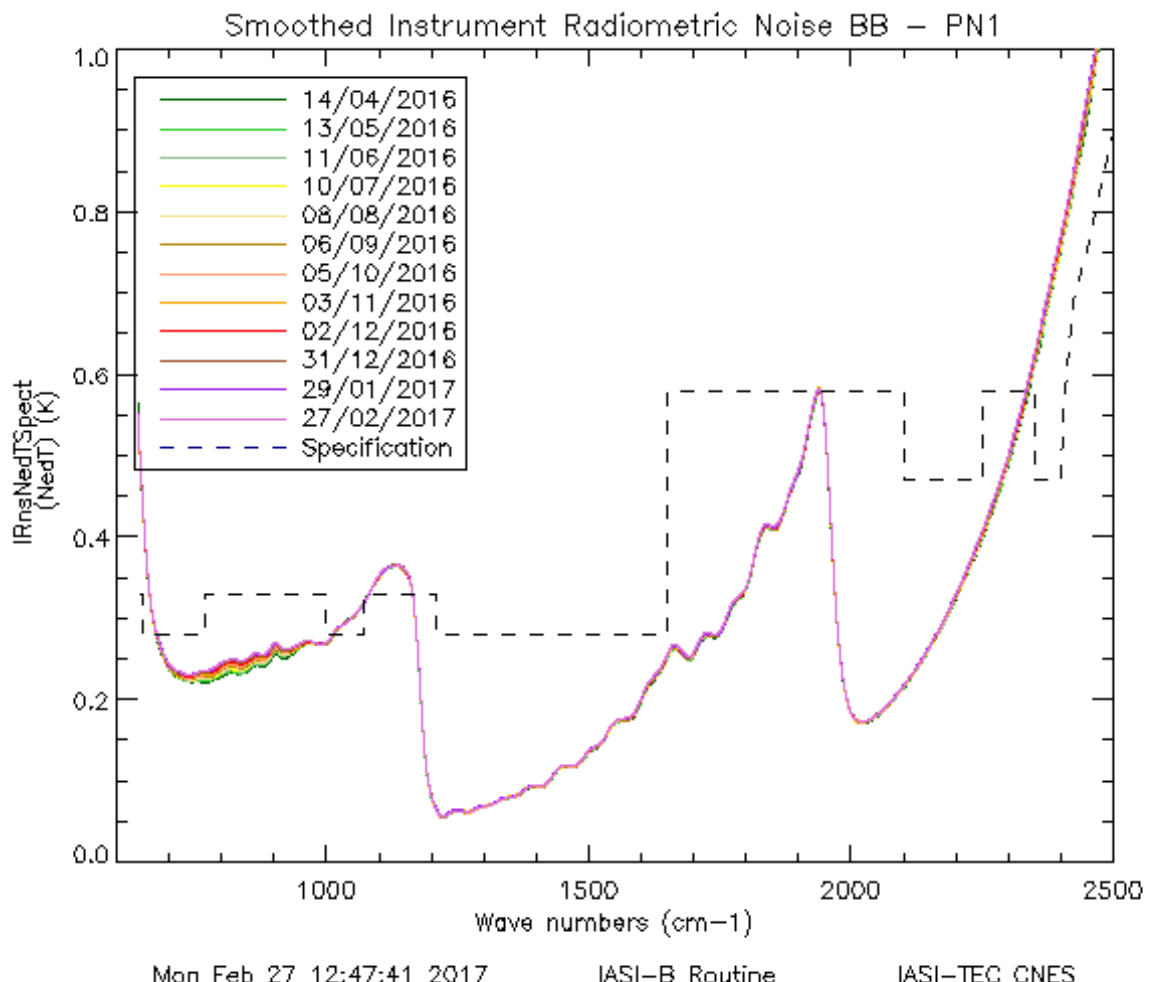


Figure 21 : Instrument noise evolution between start and end of the period

The instrument noise is very stable apart from ice effect between 700 and 1000 cm^{-1} . This point will be developed in section 4.5.4.1.

4.5.2 Radiometric Calibration

The radiometric calibration allows to convert an instrumental measurement into a physical value. The radiometric calibration is used to convert an interferogram into an absolute energy flux by taking into account instrument discrepancies. Even if the calibration has been studied on ground, it has to be continuously monitored in-flight in order to follow any potential degradation of the instrument (optics, detectors ...).

Approach: Radiometric fine characterization has been done during on-ground testing and Cal/Val. All parameters likely to cause a failure in radiometric calibration process have been identified and are continuously monitored. As long as they remain stable, there is no problem with radiometric calibration.

Evolution of scanning mirror reflectivity

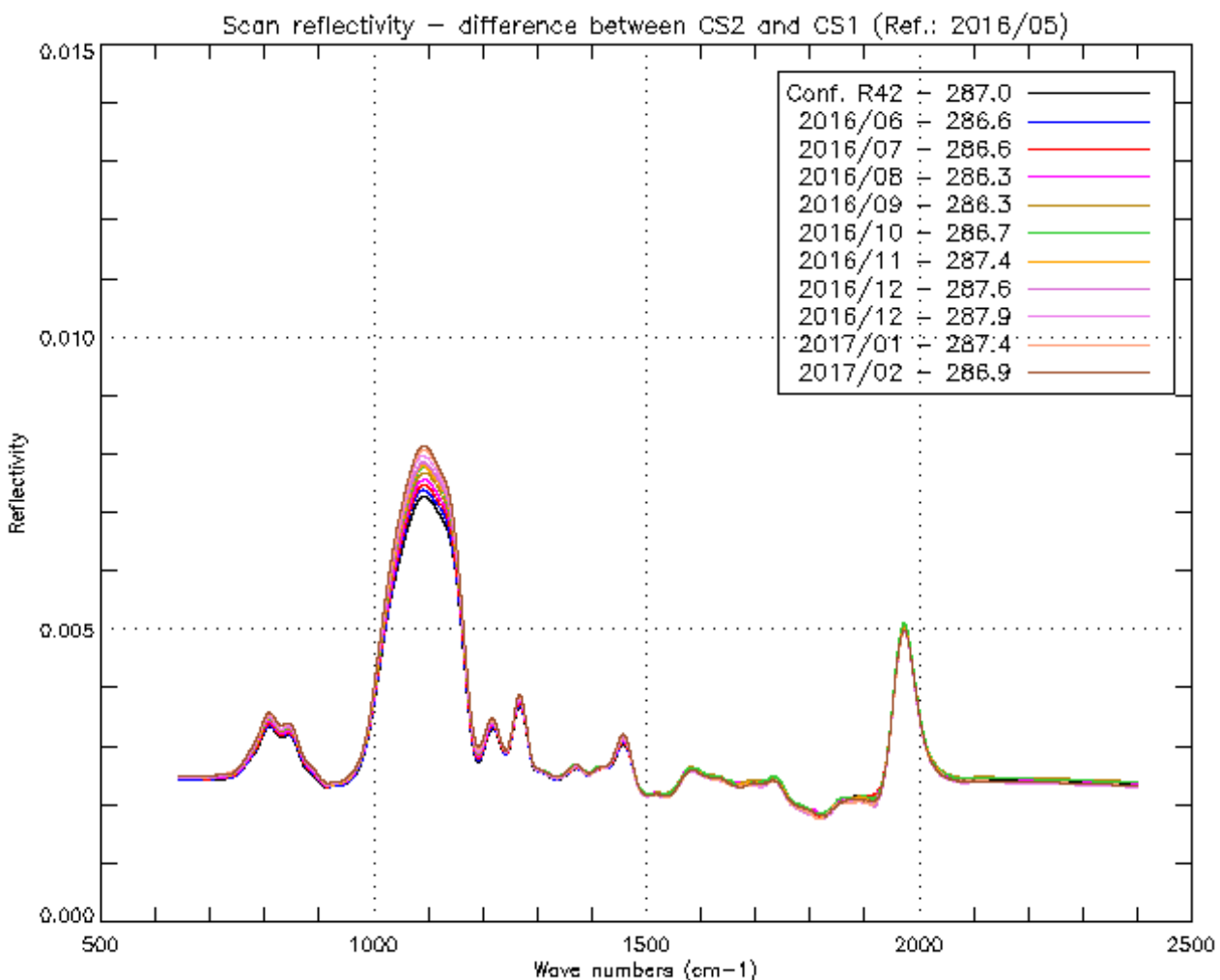


Figure 22 : Scan mirror reflectivity evolution

The reference reflexivity (in black) is the one computed on external calibration data from May 13th 2016. We see a slight evolution within [1000-1100 cm⁻¹] band. Values for wavenumbers greater than 2400 cm⁻¹ are not significant because of instrument noise.

| | | |
|---|---|---|
|  |  | Doc n°: IA-RP-2000-4332-CNE Issue: 1.0 Date: 2017-07-25 Sheet: 36 Of: 60 |
|---|---|---|

The next figure shows the translation of scan mirror reflectivity in terms of maximum radiometric calibration error for different scene temperatures.

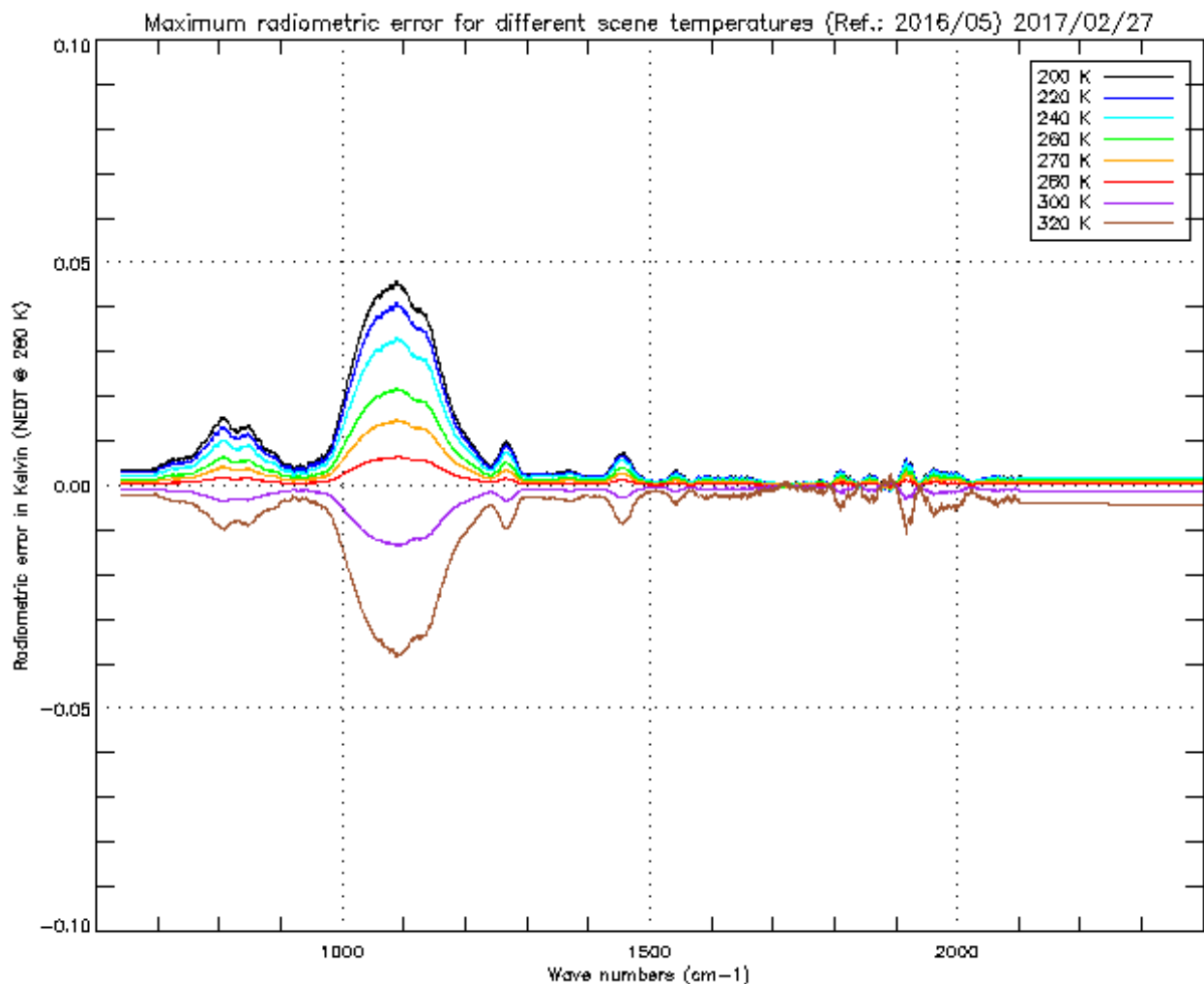


Figure 23 : Radiometric calibration error due to scan mirror reflectivity dependency with viewing angle Maximum effect on SNI for different scene temperature.
Done with the period May 16 / Feb 17

In any cases radiometric calibration maximum error is lower than the specification (0.1K). The scan mirror reflectivity law (on ground configuration), prepared with May 13th routine External Calibration data, has been updated in the operational ground segment on June 28th 2016.

| | | |
|---|---|---|
|  |  | Doc n°: IA-RP-2000-4332-CNE Issue: 1.0 Date: 2017-07-25 Sheet: 37 Of: 60 |
|---|---|---|

Internal black body

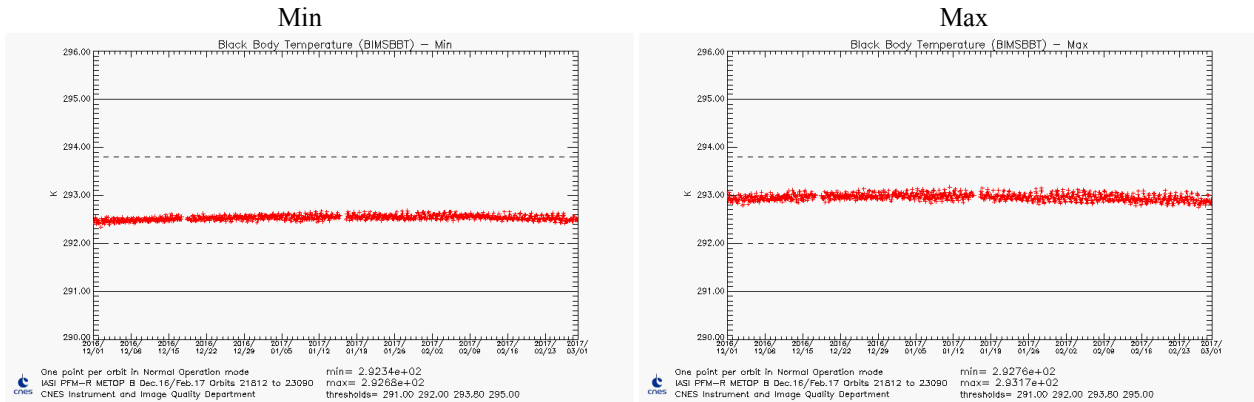
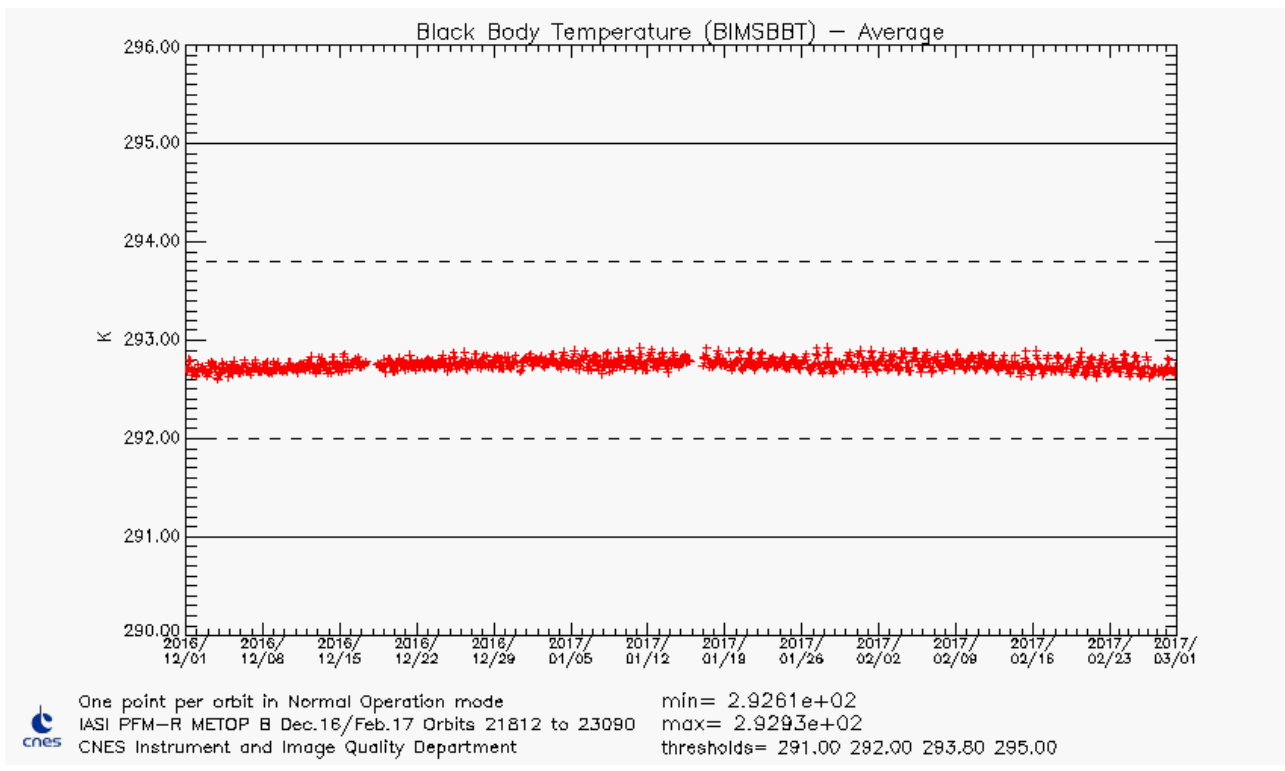


Figure 24 : Black Body Temperature

The black body temperature is stable.

| | | |
|---|---|---|
|  |  | Doc n°: IA-RP-2000-4332-CNE Issue: 1.0 Date: 2017-07-25 Sheet: 38 Of: 60 |
|---|---|---|

Non linearity of the detection chains

Non-linearity tables of the detection chains are still nominal as long as sounder focal plane temperature variation amplitude is lower than 1K.

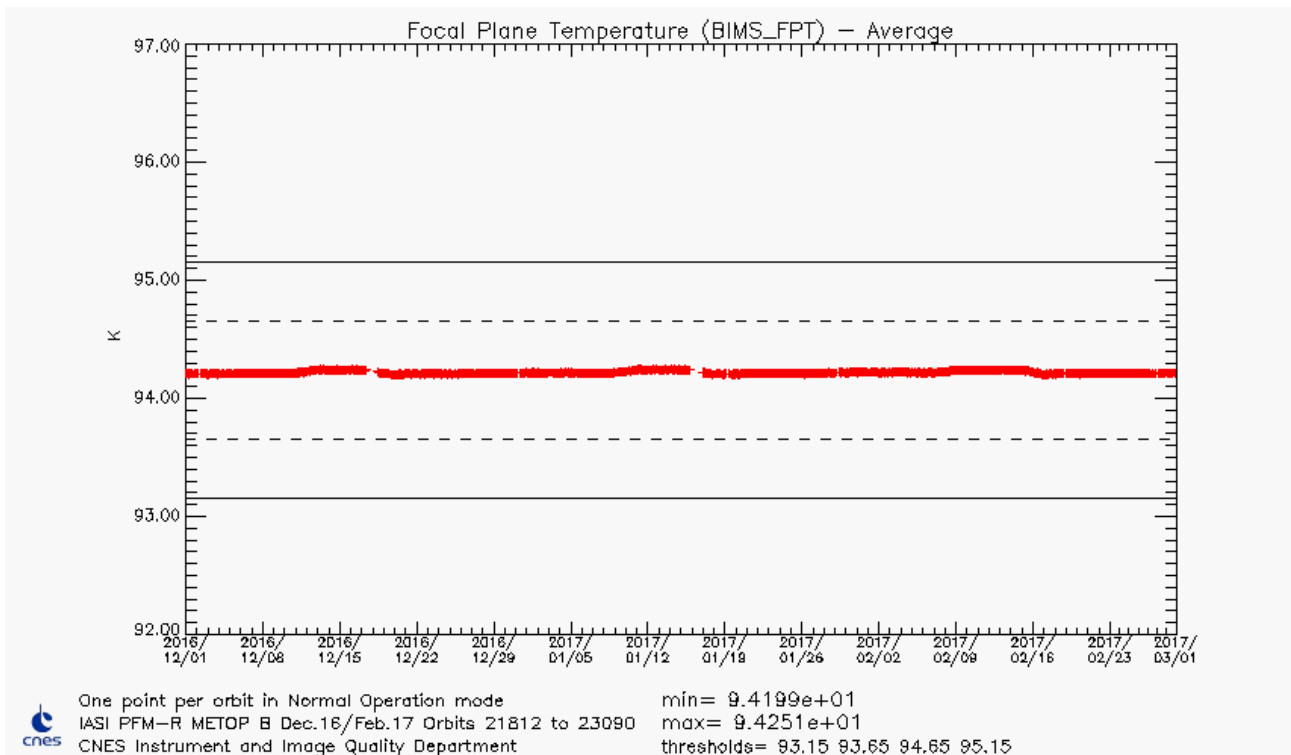


Figure 25 : Focal Plane Temperature

4.5.3 Delay of Detection Chains

Long term stability and values lower than 400 ns are required in order to properly take into account cube corner velocity fluctuations.

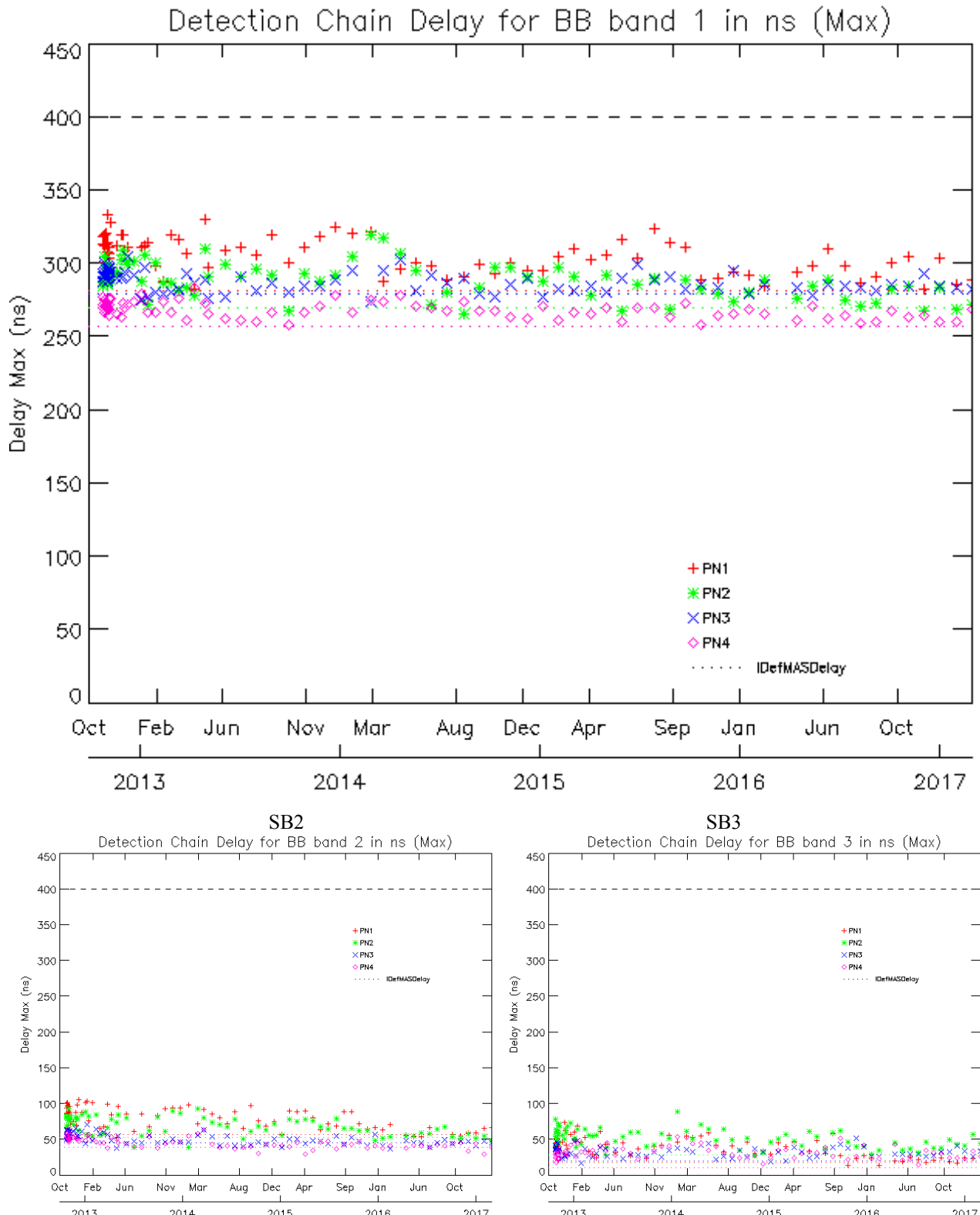


Figure 26 : Monitoring of detection chain maximum delays for all bands

4.5.4 Optical Transmission

4.5.4.1 Ice

The IASI interferometer and optical bench are regulated at 20°C temperature, while the cold box containing cold optics and detection subsystem is at about -180°C. Water desorption from the instrument causes ice formation on the field lens at the entrance of IASI cold box. This desorption phenomenon is particularly important at the beginning of the instrument in-orbit life. That's why one of the very first activities of IASI in-orbit commissioning was an outgassing phase consisting in heating the cold box up to 300 K during 20 days (from 22nd September 2012 until 16th October 2012). This operation allows removing most of the initial contaminants coming from IASI and other MetOp instruments. A routine outgassing is then needed from time to time to remove ice contamination, but less and less frequently as the desorption process becomes slower.

The first routine outgassing procedure (shorter duration and at 200K) was done from 10th to 14th March 2014.

The second routine outgassing procedure (shorter duration and at 200K) was done from 25th to 30th November 2015.

The maximum acceptable degradation of transmission is about 20% loss at 850 cm⁻¹ (which corresponds to an ice deposit thickness of about 0.5 µm).

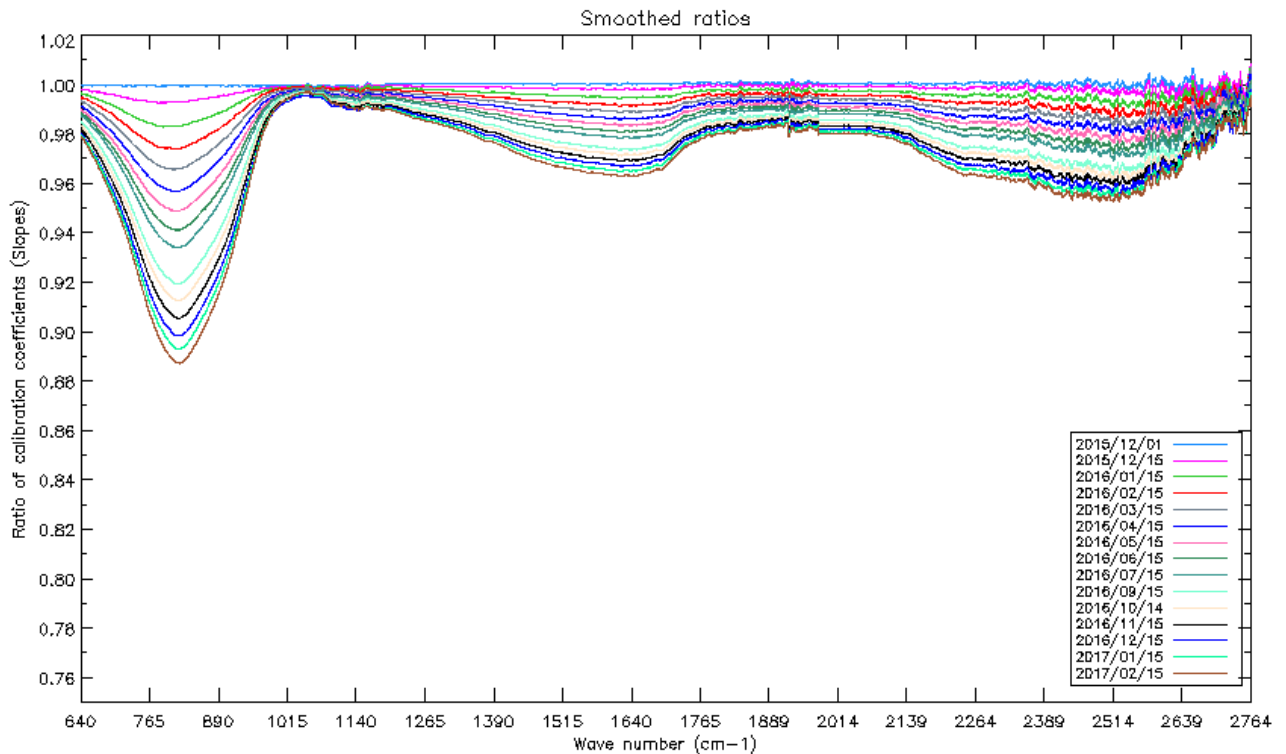


Figure 27 : Ratio of calibration coefficient slopes as a function of wave number and time after the last decontamination

| | | |
|---|---|---|
|  |  | Doc n°: IA-RP-2000-4332-CNE Issue: 1.0 Date: 2017-07-25 Sheet: 41 Of: 60 |
|---|---|---|

4.5.4.2 Prediction of decontamination date

The transmission degradation rate is regularly monitored by CNES TEC through gain measurements given by calibration coefficients ratios.

The loss of instrument gain due to ice contamination is, as expected, decreasing over time. The next decontamination is not expected before mid of 2018.

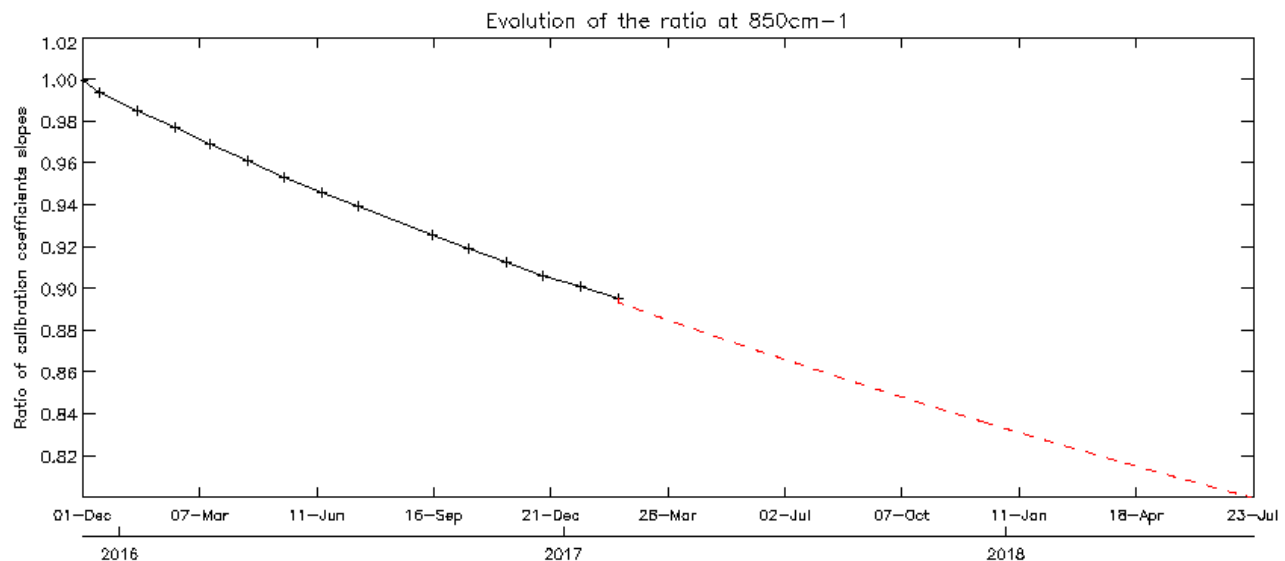


Figure 28 : Temporal evolution of calibration ratio coefficient slopes since the last decontamination. The curve was fitted with a decreasing exponential function to determine a rough date for the next decontamination (relative gain evolution of 0.8)

| | | |
|---|---|-----------------------------|
|  |  | Doc n°: IA-RP-2000-4332-CNE |
| | | Issue: 1.0 |
| | | Date: 2017-07-25 |
| | | Sheet: 42 Of: 60 |

4.5.5 Interferometric Contrast

The interferometric contrast is defined as the interferogram fringe discrimination power. Figure 29 shows temporal evolution of instrument contrast since the beginning of IASI life in orbit for all pixels and all CCD.

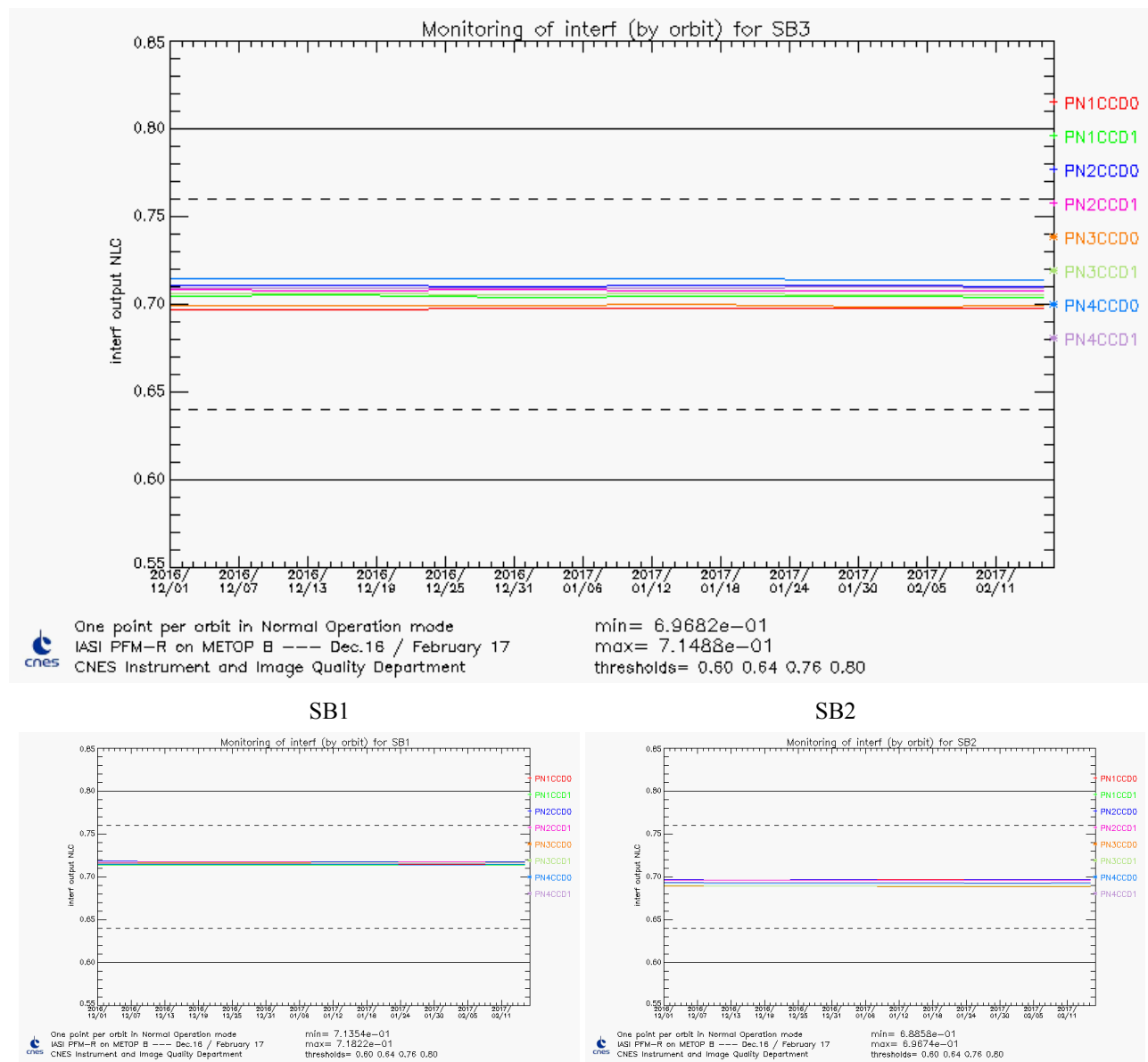


Figure 29 : Contrast Monitoring

| | | |
|---|---|---|
|  |  | Doc n°: IA-RP-2000-4332-CNE Issue: 1.0 Date: 2017-07-25 Sheet: 43 Of: 60 |
|---|---|---|

4.5.6 Interferogram Baseline

The interferogram baseline is the mean value of the interferogram. Figure 30 shows temporal evolution of the baseline of the raw interferograms on calibration targets (BB and CS). The values are raw values, they are not physical, but the evolution is interesting: as the values are proportional to the energy received from a target and calibration targets are stable, the evolution can show the decrease of instrument transmission or events due to energetic particles.

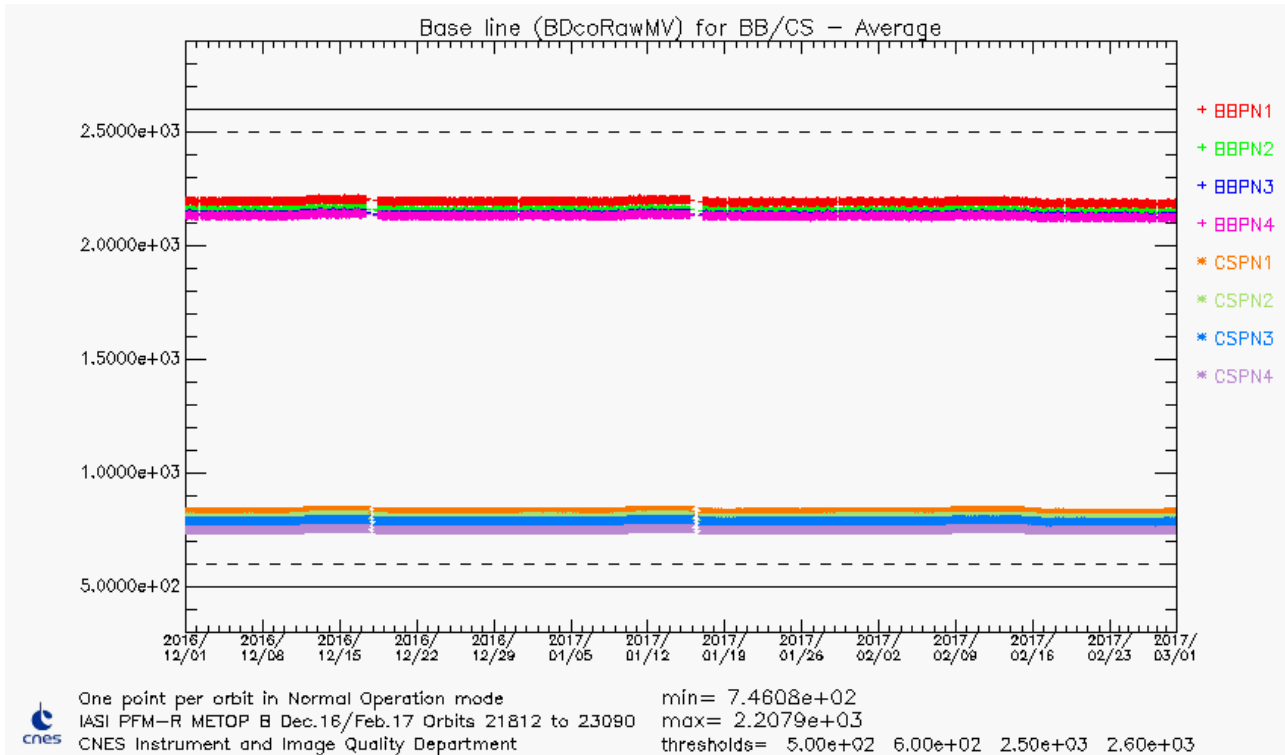


Figure 30 : Monitoring of interferogram baseline

| | | |
|---|---|-----------------------------|
|  |  | Doc n°: IA-RP-2000-4332-CNE |
| | | Issue: 1.0 |
| | | Date: 2017-07-25 |
| | | Sheet: 44 Of: 60 |

4.5.7 Detection Chain

Detection chains are tuned in gain and offset via telecommand. The goal is to avoid saturation while conserving the maximum dynamic to limit digitalization noise.

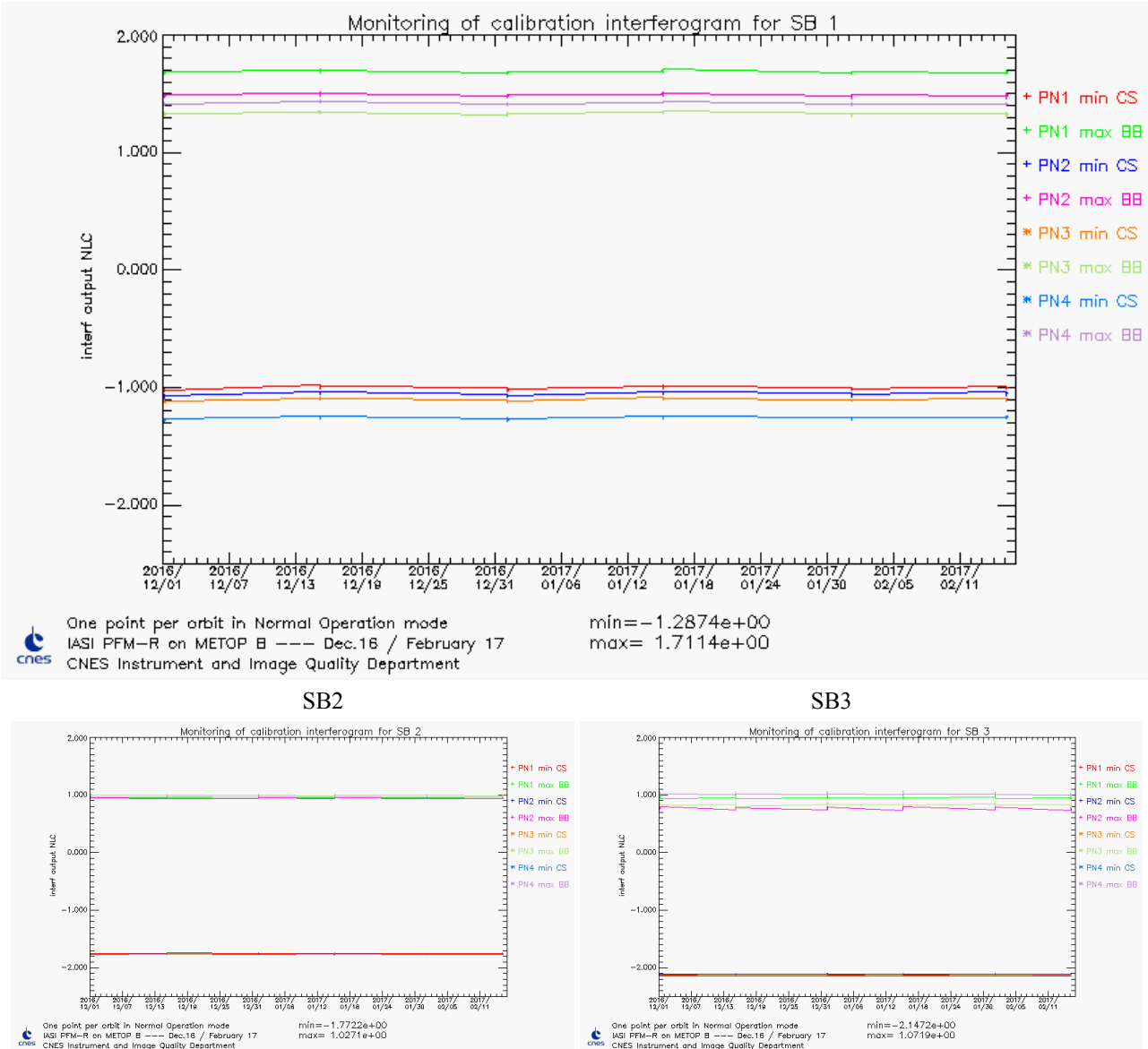


Figure 31 : Monitoring of detection chain margins

Margins are sufficient for the moment. The slight decreasing slope in SB1 (BB) for all pixels is linked to the instrument transmission evolution already mentioned in §4.5.4.1.

4.5.8 Conclusion

The radiometric performances of IASI are nominal and stable. An extrapolation of the current calibration ratio leads to a rough date for the next decontamination mid 2018. Scan mirror reflectivity was updated in June 2016. The next update is not foreseen before autumn 2017.

| | | |
|---|---|-----------------------------|
|  |  | Doc n°: IA-RP-2000-4332-CNE |
| | | Issue: 1.0 |
| | | Date: 2017-07-25 |
| | | Sheet: 45 Of: 60 |

4.6 SOUNDER SPECTRAL PERFORMANCES

The goal of the spectral calibration is to provide the best estimates of spectral position of the 8461 IASI channels.

The large sensitivity of infrared spectrum to spectral calibration errors has led to stringent specifications:

- A prior knowledge of spectral position better than of 2.10^{-4} (design)
- A posterior maximum spectral calibration relative error of 2.10^{-6} (after calibration by OPS)

In order to reach the specification of 2.10^{-6} , we need an accurate Instrument Spectral Response Function (ISRF) model. This model have been done and validated in the early time of IASI development.

For sake of operational time constrain, complete ISRF calculation is not done in real-time by OPS software but pre-calculated and stored in a database called “spectral database”. OPS processing determine on-line the most relevant instrument function to be used by OPS with respect to current values of a set of parameters (interferometric axis, cube corner offset...).

The approach to monitor IASI spectral performances is very similar to the one used for radiometric calibration. Spectral calibration fine characterization has been done during ground testing and Cal/Val. All parameters likely to cause a failure in spectral calibration process have been identified and are continuously monitored. As long as they remain stable, there is no problem with IASI spectral calibration.

In addition, a spectral calibration assessment is done over homogeneous scenes when IASI is in external calibration, nadir view.

Since the permanent compensation device stop on 7th October 2015, the monitoring of the ghost was cancelled as the data are no more affected by the ghost.

4.6.1 Monitoring of the ISRF inputs

4.6.1.1 Position of the interferometric axis

The interferometric axis is the cube corner displacement direction. Its value has changed several times during CalVal due to the various configurations used. Since the end of CalVal, its value is now stable around ($Y = 1060\mu\text{rad}$; $Z = 1210\mu\text{rad}$). The central position used in the “spectral database” generation, are $1000\mu\text{rad}$ and $1200\mu\text{rad}$, respectively for Y and Z axis.

Since the drift of the interferometer axis is lower than $300\mu\text{rad}$, there is no need to update the “spectral database”.

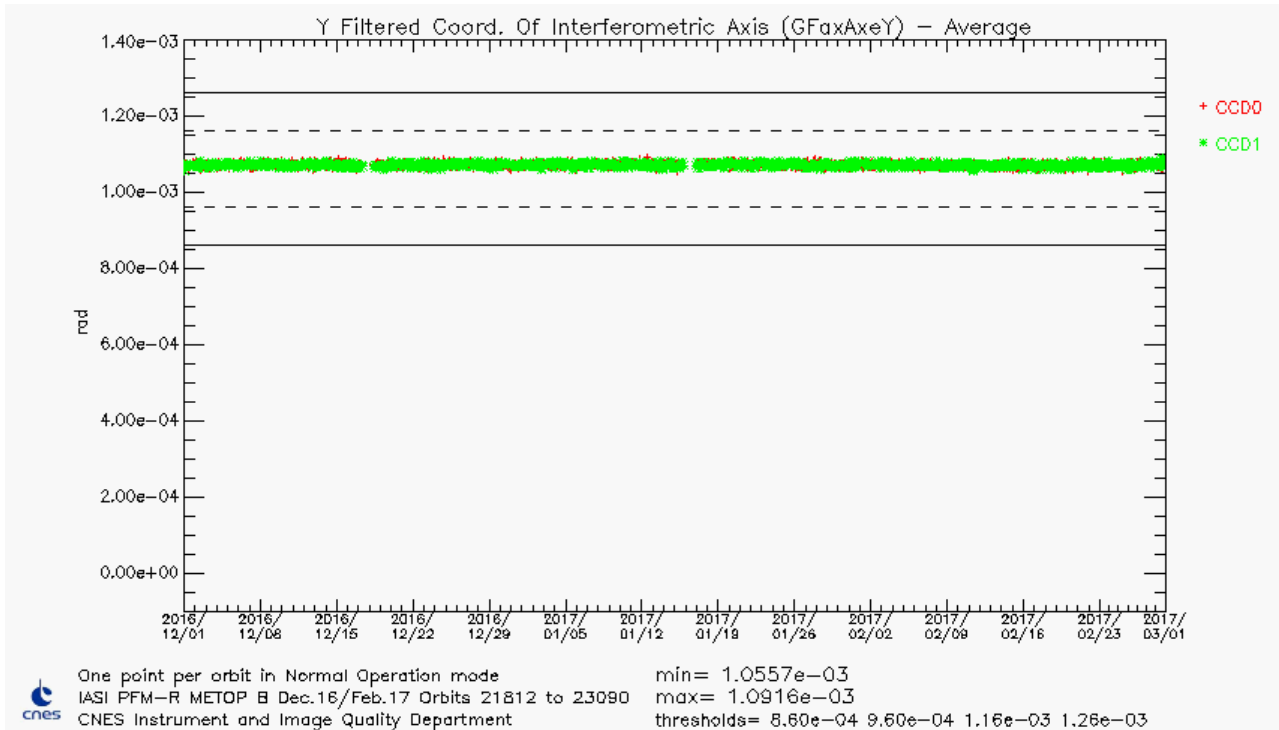


Figure 32 : GFaxAxeY average (Y filtered coordinates of sounder interferometric axis)

| | | |
|---|---|---|
|  |  | Doc n°: IA-RP-2000-4332-CNE Issue: 1.0 Date: 2017-07-25 Sheet: 46 Of: 60 |
|---|---|---|

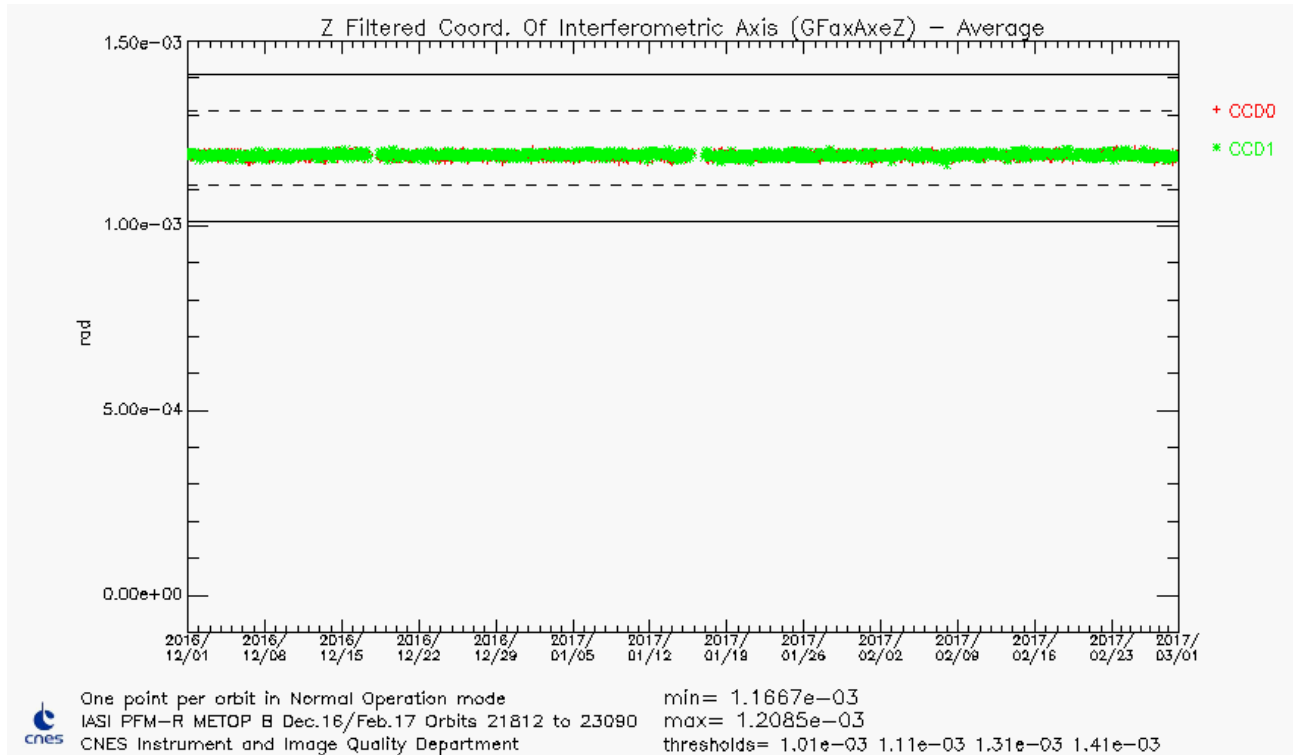


Figure 33 : GFaxAxeZ average (Z filtered coordinates of sounder interferometric axis)

4.6.1.2 Cube Corner constant offset

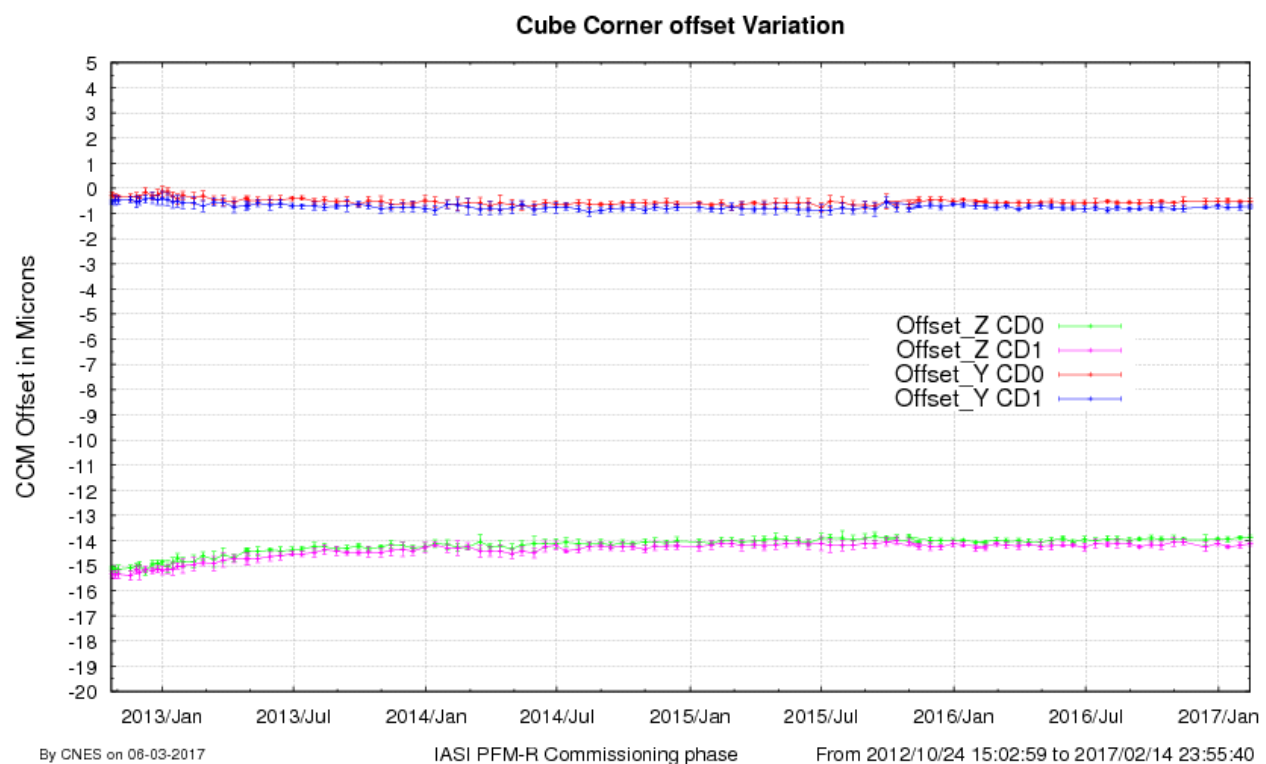


Figure 34 : Cube Corner offset variation

| | | |
|---|---|---|
|  |  | Doc n°: IA-RP-2000-4332-CNE Issue: 1.0 Date: 2017-07-25 Sheet: 47 Of: 60 |
|---|---|---|

Reference cube corner offsets, used in the spectral database of the period (ODB 12), are $-0.48 \mu\text{m}$, $-0.61 \mu\text{m}$, $-14.54 \mu\text{m}$ and $-14.64 \mu\text{m}$, respectively for Y CD0, Y CD1, Z CD0 and Z CD1. Since the drift of cube corner offset is lower than $4 \mu\text{m}$, there is no need to update the spectral database.

4.6.1.3 Cube corner velocity

Refer to REVEX, paragraph 5.5.

4.6.1.4 Interferometer optical bench temperature

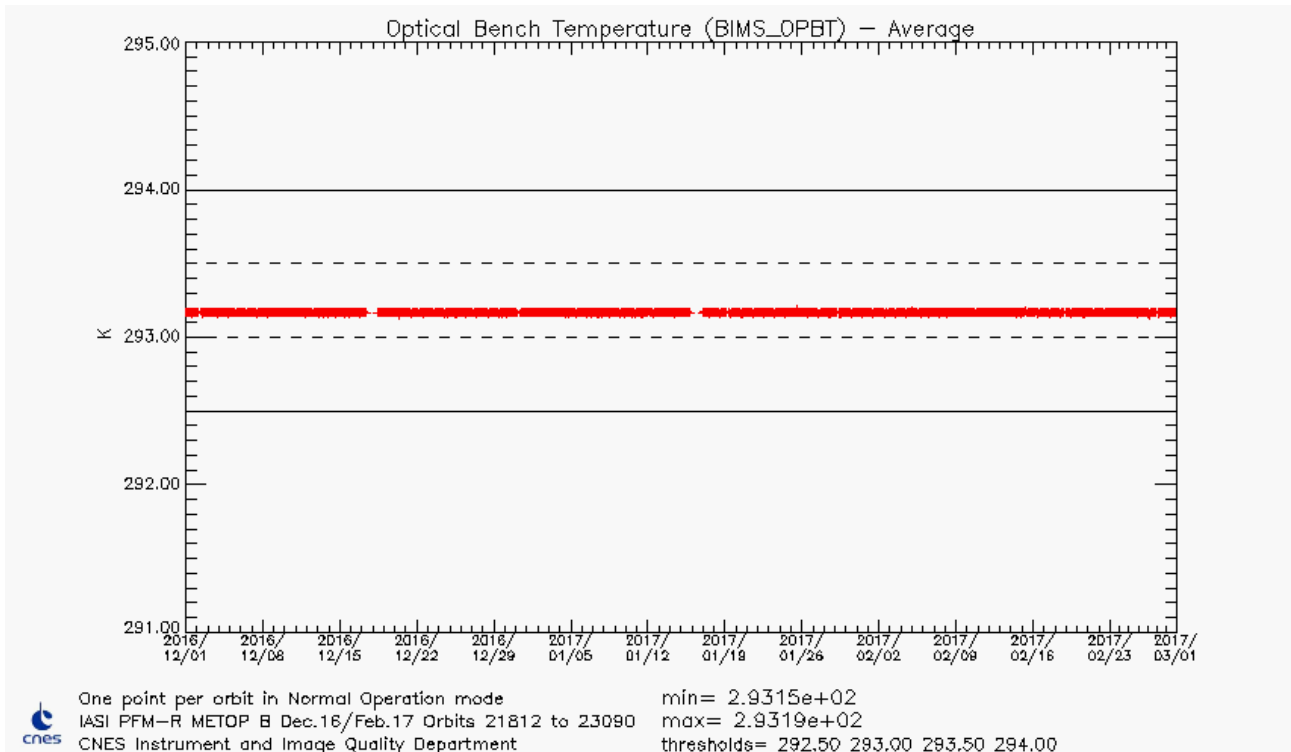


Figure 35 : Optical bench Temperature

4.6.2 Spectral calibration assessment

Absolute spectral calibration assessment and Interpixel spectral calibration assessment are performed during routine External Calibration on Earth views at nadir (SP 15) and synthesized once a year.

Refer to REVEX, paragraph 6.6.2.

4.6.3 Conclusion

All parameters impacting IASI spectral calibration are stable and within specifications.

| | | |
|---|---|-----------------------------|
|  |  | Doc n°: IA-RP-2000-4332-CNE |
| | | Issue: 1.0 |
| | | Date: 2017-07-25 |
| | | Sheet: 48 Of: 60 |

4.7 GEOMETRIC PERFORMANCES

The geometric calibration is performed on ground (level 1 processing). Most of the analyses of geometric performances require being in external calibration mode.

Specifications are the following: the IIS/AVHRR co-registration has to be better than 0.3AVHRR pixel while the IIS/sounder co-registration has to be better than 0.8mrad.

4.7.1 Sounder / IIS co-registration monitoring

This monitoring is performed one time a year, generally around September for REVEX and march for mid-REVEX.

The sonder/IIS coregistration error is lower than 100μrad (eq. 100m on ground).

4.7.2 IIS / AVHRR co-registration

The IIS/AVHRR co-registration is permanently estimated by the L1 processing chain.

Note that AVHRR channels 4 and 5 are within the IIS spectral filter. The spatial resolution of the IIS (0,7km) is close to AVHRR (1km).

The IIS/AVHRR offset guess in the ground segment configuration is used when the algorithm of correlation between IIS and AVHRR does not converge (typically over homogeneous scenes).

The following figures show a comparison of IIS-AVHRR offsets (GIacOffsetIISAvhrr) mean profiles.

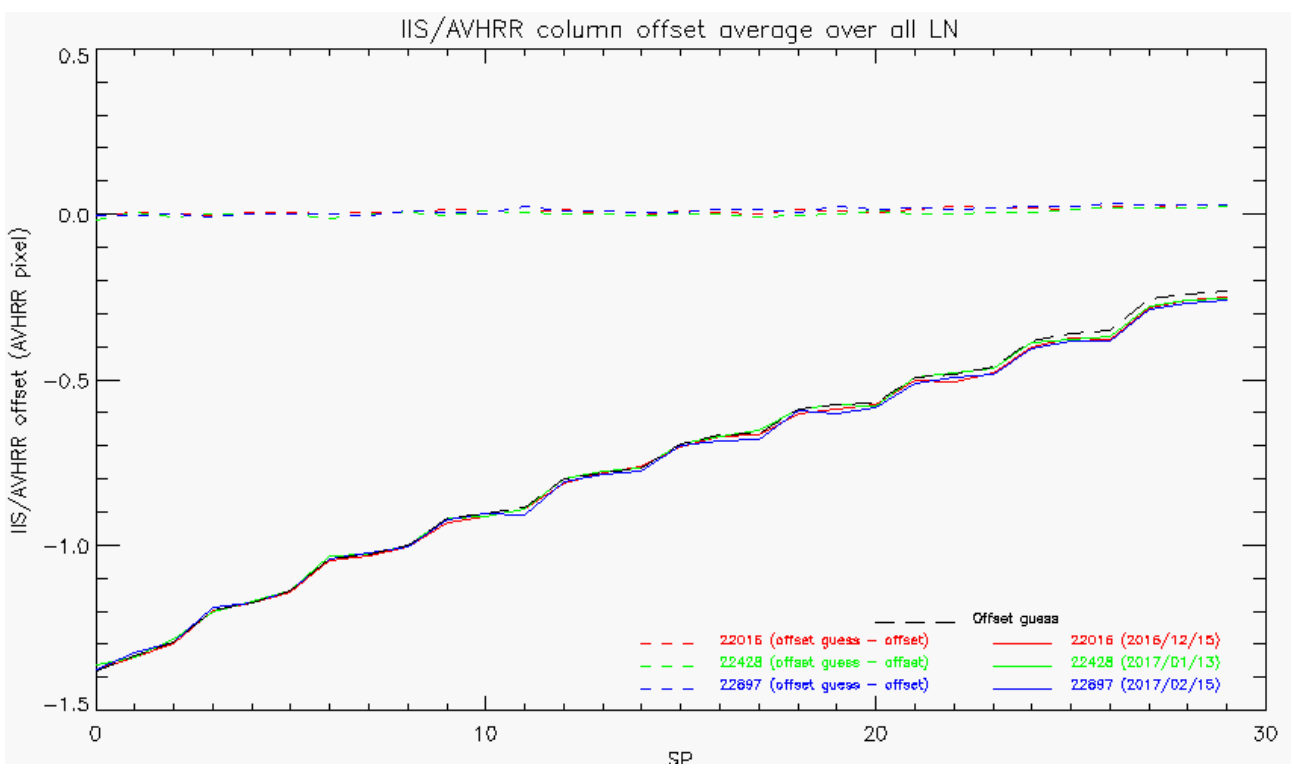


Figure 36 : Column offset (black) guess vs. column offset averaged over all lines (LN) as a function of the scan position (SP=SN), and orbit number

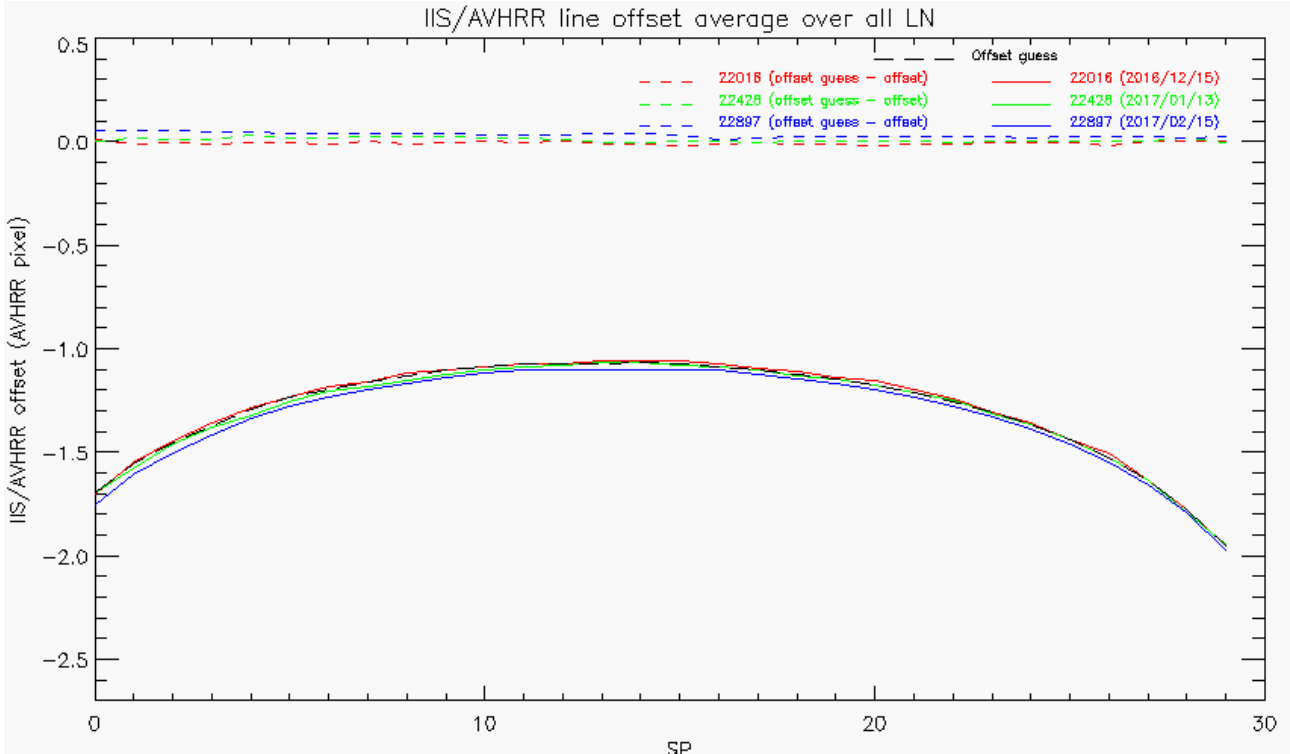


Figure 37 : Line offset guess (black) vs. line offset averaged over all lines (LN) as a function of the scan position (SP=SN), and the orbit number

For both across track and along track, the residuals between measured and IIS/AVHRR offset guess in the ground segment configuration are lower than 0.1 AVHRR pixel for all viewing angles, that is equivalent to 100m on ground.

The values are stable.

4.7.3 Conclusion

The positions of IASI pixel are considered stable and well within specification.

IIS-sounder co-registration is stable at about 100 μ rad which is equivalent to 100m on ground (specification : < 0.8 mrad).

IIS-AVHRR offset is lower than two pixels and stable over time: less than 0.1 AVHRR pixels over three months (specification: < 0.3 AVHRR pixel).

IASI pixel centre location accuracy in AVHRR raster is around 200m. The geolocation of IASI pixels are thus considered stable and well within specification (5 km).

| | | |
|---|---|---|
|  |  | Doc n°: IA-RP-2000-4332-CNE Issue: 1.0 Date: 2017-07-25 Sheet: 50 Of: 60 |
|---|---|---|

4.8 IASI-B INTER-CALIBRATION WITH IASI-A, CRIS AND AIRS

The objective of the radiometric and spectral inter-calibration between IASI-B, IASI-A, CRIS and AIRS is to perform an external monitoring of the IASI performances and to ensure the consistency of the hyperspectral TIR sensors and in particular the continuity of the IASI mission. We aim here at checking the performance of the radiometric absolute calibration accuracy of 0.5K per IASI channel, and of the spectral absolute calibration accuracy of 2 ppm.

The inter-calibration is performed with the SIC software. The methodology is described in the technical note DA.2. Roughly, the methodology is based on the construction of a database in which each data is the difference IASI-B – IASI-A, IASI-B – CRIS or IASI-B – AIRS over a common observation made by both sounders. “Common” means same place, same time and same viewing conditions so that the only difference is not geophysical but due to a calibration bias. Statistics over this database emphasize the radiometric and spectral biases.

4.8.1 IASI-B inter-calibration with IASI-A

For IASI-B / IASI-A, the common observations are the overlapping areas between two consecutive orbits of MetOp-A and MetOp-B. They always exhibit a temporal gap of ~50 min between IASI-A and B (with the two cases “A before B” and “A after B”), and the geometries of the observations are different and generally off-nadir with opposite angles. These two drawbacks are minimized by a pre-filtering performed to only use the most stable and homogeneous scenes, using the geolocation, Cld_AVHRR and ECMWF information. Each scene is then a regional averaging of the soundings. The comparison is performed at native spectral resolution.

Figure 38 gives the mean and standard deviation of $\Delta T @ 280K$ for one year of data. We see that IASI-A and IASI-B are very well cross-calibrated, with biases lower or equal to 0.1K in absolute value. For information, we checked that the distribution of the surface temperature of the scenes in the database covers a large range (from 220K to 280K).

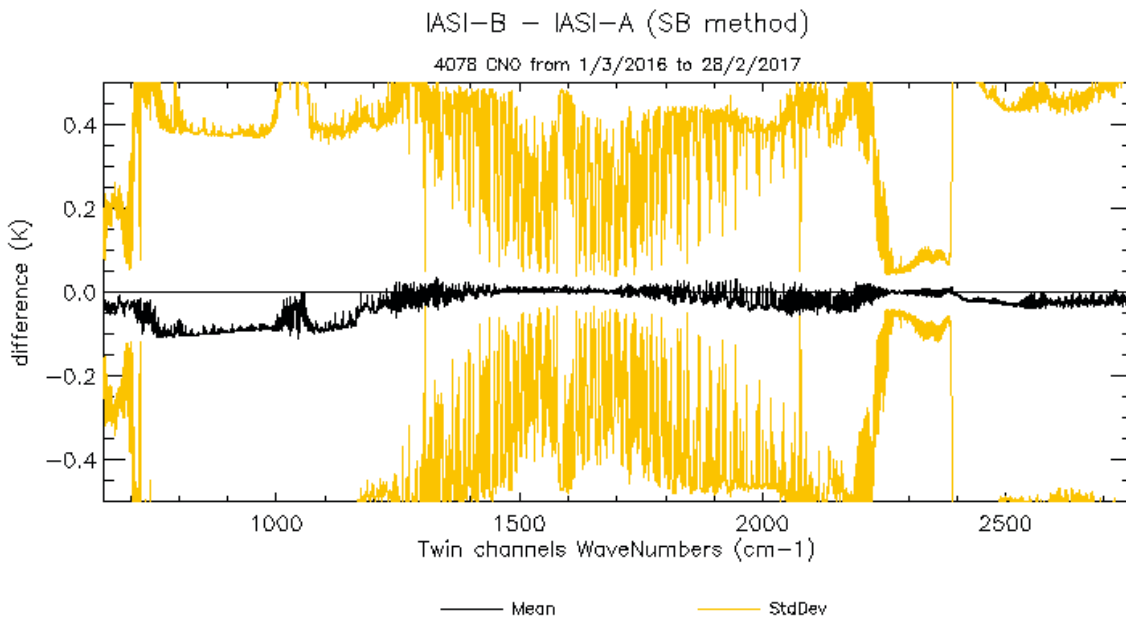


Figure 38 : Mean (black curve) and standard deviation (yellow) of the difference in brightness temperature IASI-B – IASI-A

Figure 39 shows the temporal evolution of three broad pseudo-channels, corresponding approximately to the IASI bands 1, 2 and 3 (more precisely, to their overlapping with the CRIS and AIRS coverage). We see that the difference between IASI-B and IASI-A is stable with time, with slight variations in IASI B1.

| | | |
|---|---|-----------------------------|
|  |  | Doc n°: IA-RP-2000-4332-CNE |
| | | Issue: 1.0 |
| | | Date: 2017-07-25 |
| | | Sheet: 51 Of: 60 |

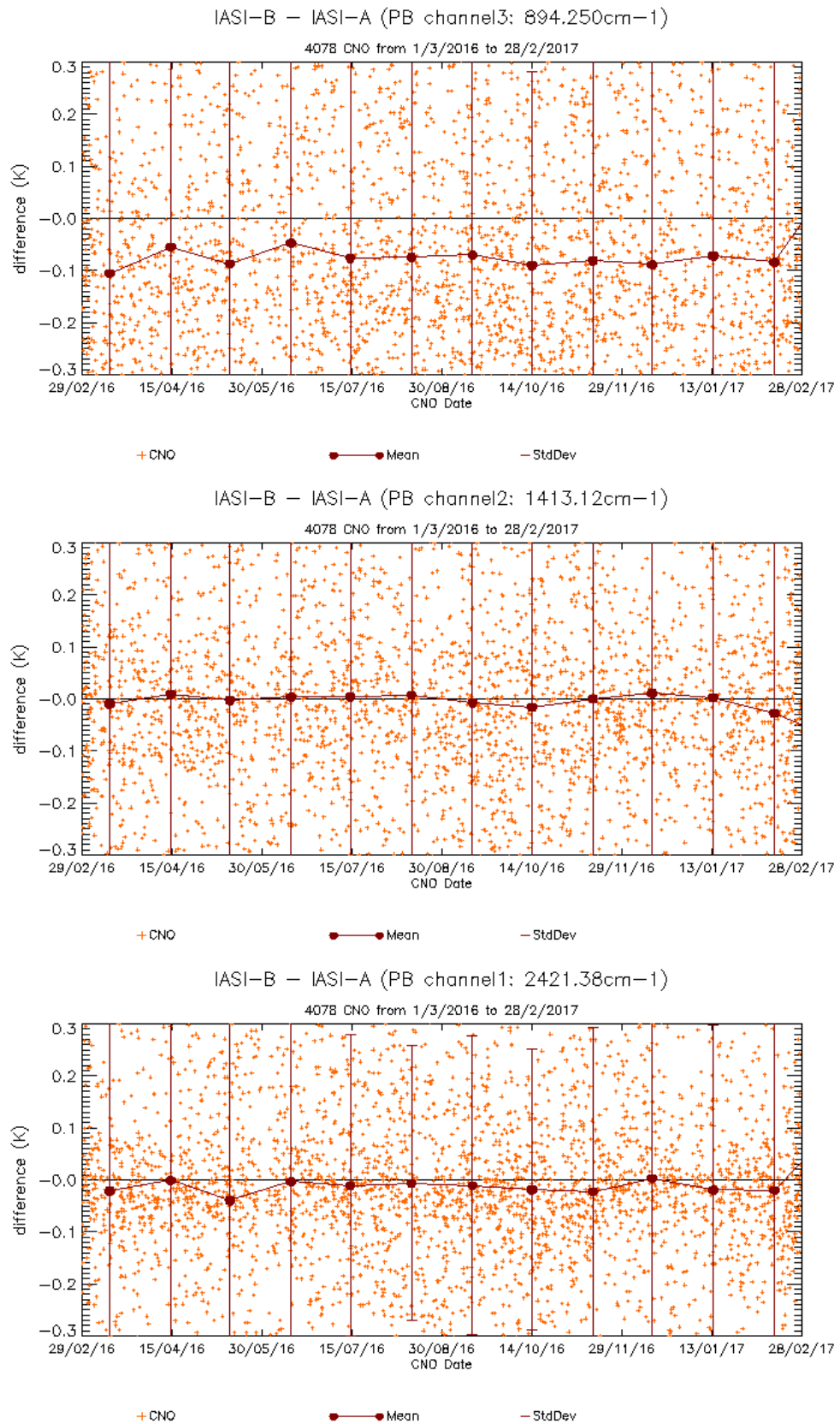


Figure 39 : Temporal evolution of differences IASI-B – IASI-A in brightness temperature spectrally integrated over the approximate three IASI bands

The spectral inter-comparison is performed on the same spectra as the radiometric inter-comparison. For each common observation, a cross-correlation of both spectra is performed in 30 small spectral windows for different spectral shifts. The maximum of correlation gives the actual spectral shifts expressed in $\Delta v/v$. Figure 40 gives the mean of $\Delta v/v$ over the complete dataset. We see that the spectral bias between IASI-B and IASI-A is lower than 1 ppm in absolute value, which is compliant with the specification of 2 ppm for most channels. The channels out of specification are due to the perturbation of the cross-correlation by noise.

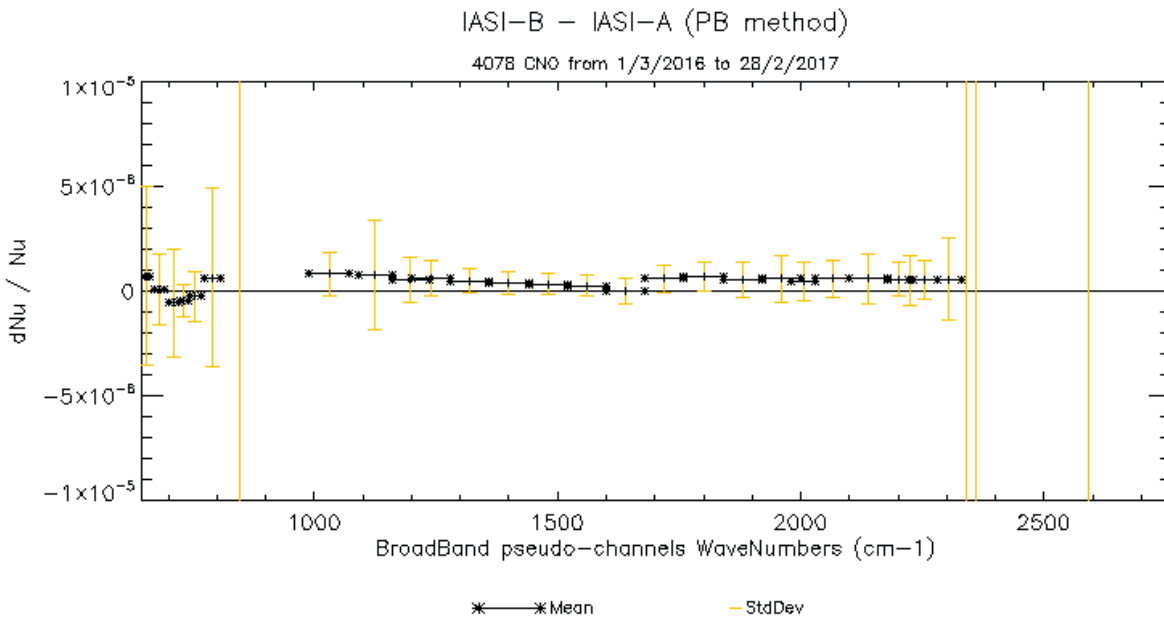


Figure 40 : Mean (black curve) and standard deviation (yellow curve) of the difference spectral calibration $\Delta v/v$ between IASI-B and A.

Figure 41 shows the temporal evolution of the difference spectral calibration $\Delta v/v$ between IASI-B and A in the spectral window centered on 2200cm $^{-1}$. We see that the IASI-A/IASI-B spectral inter-calibration is very stable.

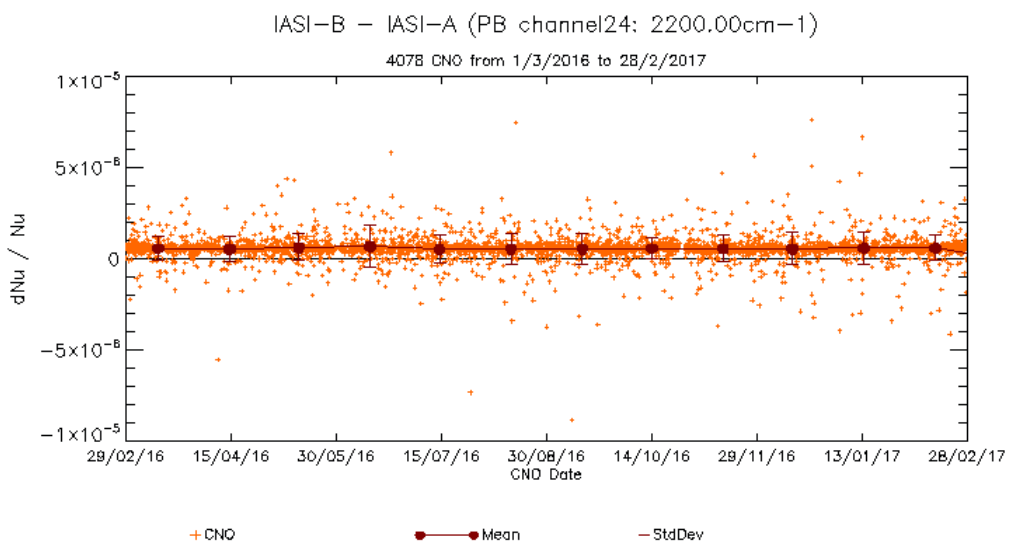


Figure 41 : Temporal evolution of the difference spectral calibration $\Delta v/v$ between IASI-B and A in the spectral window centered around 2200cm $^{-1}$.

4.8.2 IASI-B inter-calibration with CRIS

For IASI-B and CRIS, the basis of the algorithm is similar to that IASI-B / IASI-A, but now the database is filled with Simultaneous Nadir Overpasses, occurring at high latitudes (because of the differences in the local time of the orbits). Each scene is a regional averaging of the soundings, with a spectral reduction in broad pseudo-bands. Because of the differences in spectral resolution, no spectral inter-calibration is performed.

Figure 42 shows the mean and standard deviation of IASI-B - CRIS for one year of data. We see that IASI-A and CRIS are very well cross-calibrated, with biases lower or equal to 0.1K in absolute value (except for one pseudo-band).

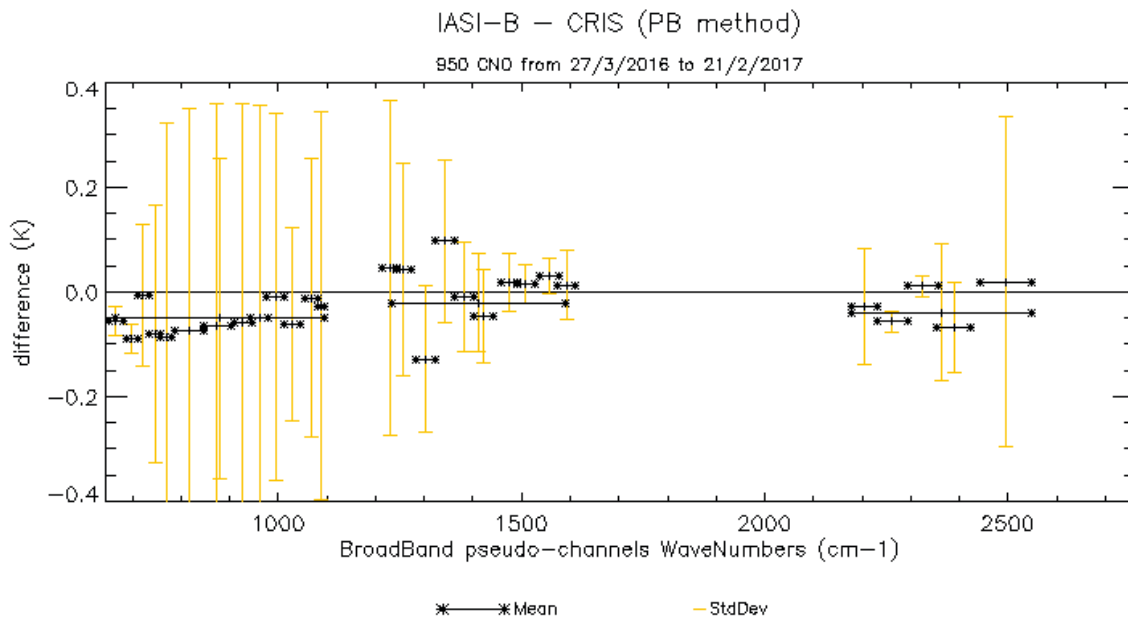


Figure 42 : Mean (black curve) and standard deviation (yellow) of the difference in brightness temperature IASI-B – CRIS

Figure 43 shows the temporal evolution of the three broadest pseudo-channels, corresponding approximately to the IASI bands 1, 2 and 3 (more precisely, to their overlapping with the CRIS coverage). We see that the difference between IASI-B and CRIS is stable with time, with slight variations in IASI B1. Note that some large temporal gaps may be encountered for IASI-B / CRIS, due to the orbital configuration and the tolerance in simultaneity, making some monthly means meaningless.

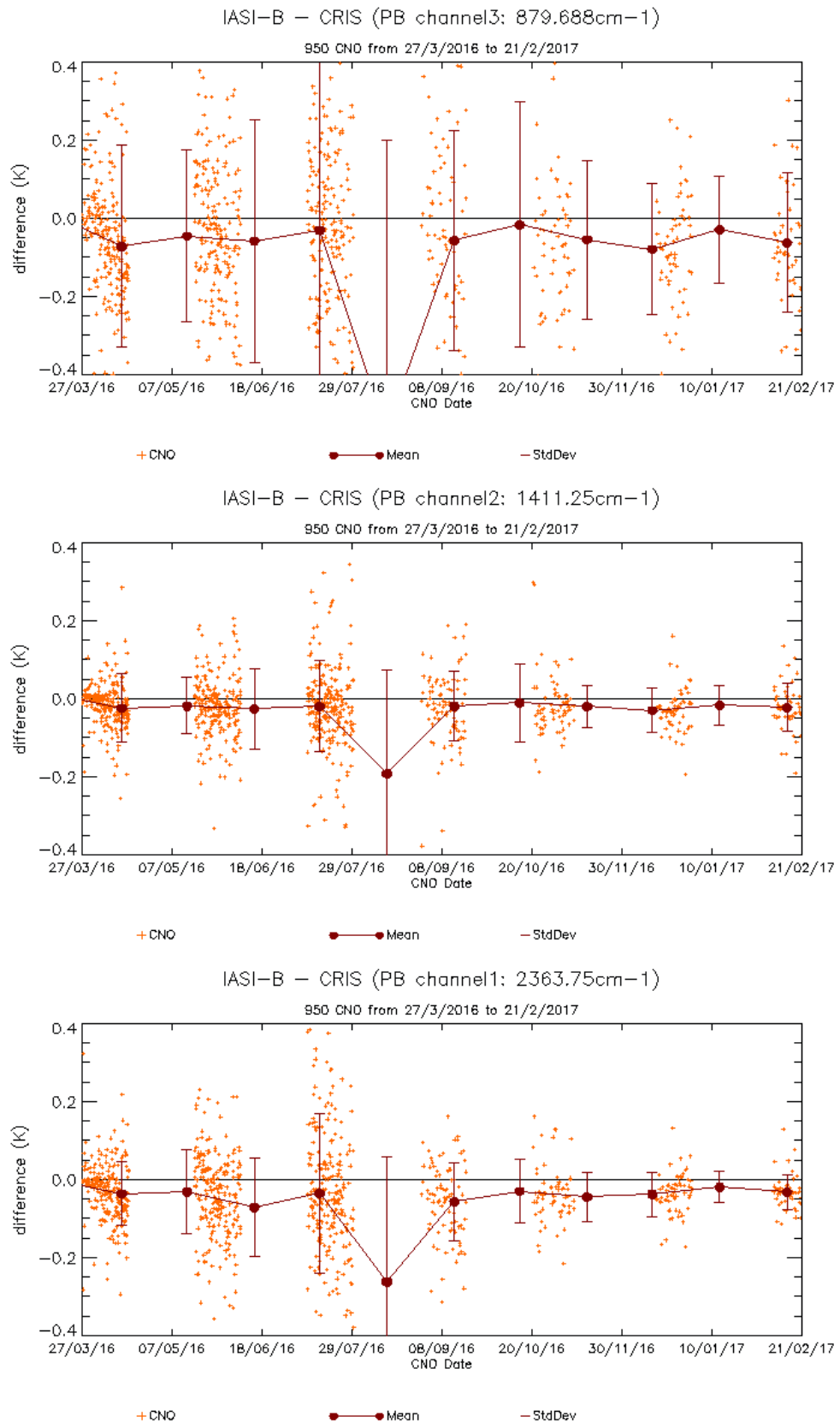
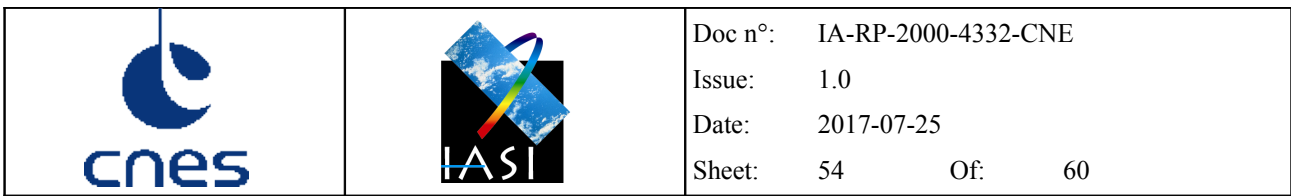


Figure 43 : Temporal evolution of the differences IASI-B – CRIS in brightness temperature over the approximate three IASI bands, with monthly means.

| | | |
|---|---|---|
|  |  | Doc n°: IA-RP-2000-4332-CNE Issue: 1.0 Date: 2017-07-25 Sheet: 55 Of: 60 |
|---|---|---|

4.8.3 IASI-B inter-calibration with AIRS

For IASI-B and AIRS, the algorithm is similar to that IASI-B / CRIS (similar orbital configuration).

Figure 44 shows the mean and standard deviation of IASI-B - AIRS for one year of data. We see that IASI-B and AIRS are very well cross-calibrated, with biases lower or equal to 0.15K in absolute value (except for one pseudo-band).

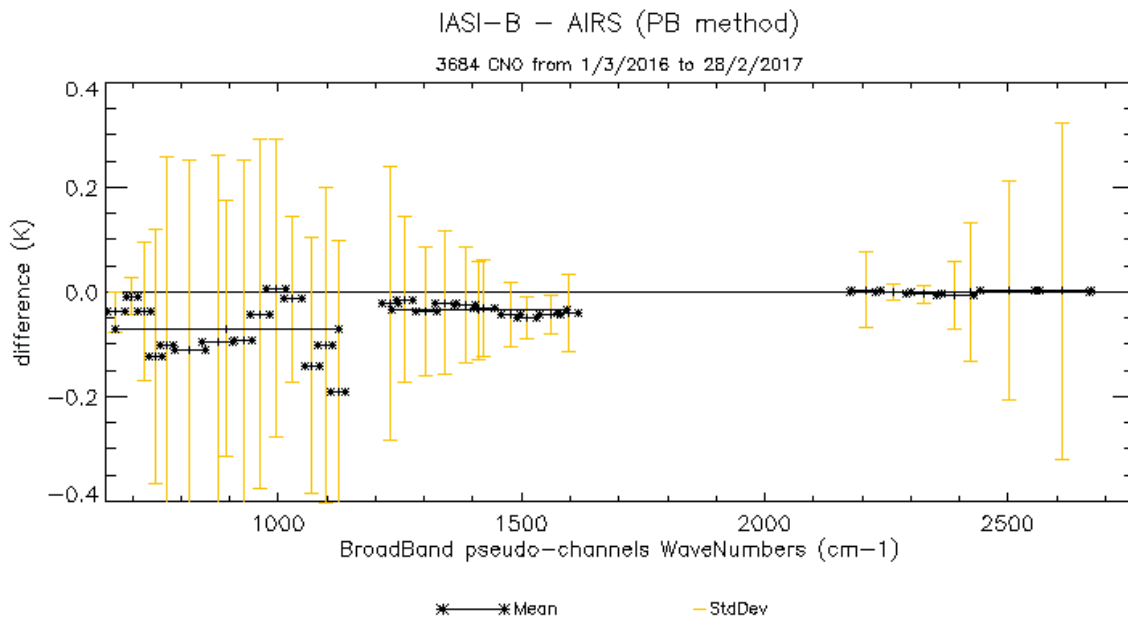


Figure 44 : Mean (black curve) and standard deviation (yellow) of the difference in brightness temperature IASI-B – AIRS.

Figure 45 shows the temporal evolution of the three broadest pseudo-channels, corresponding approximately to the IASI bands 1, 2 and 3 (more precisely, to their overlapping with the AIRS coverage). We see that the difference between IASI-B and AIRS is very stable with time, even more than IASI-B - CRIS. For IASI-B / AIRS no large temporal gaps are observed.

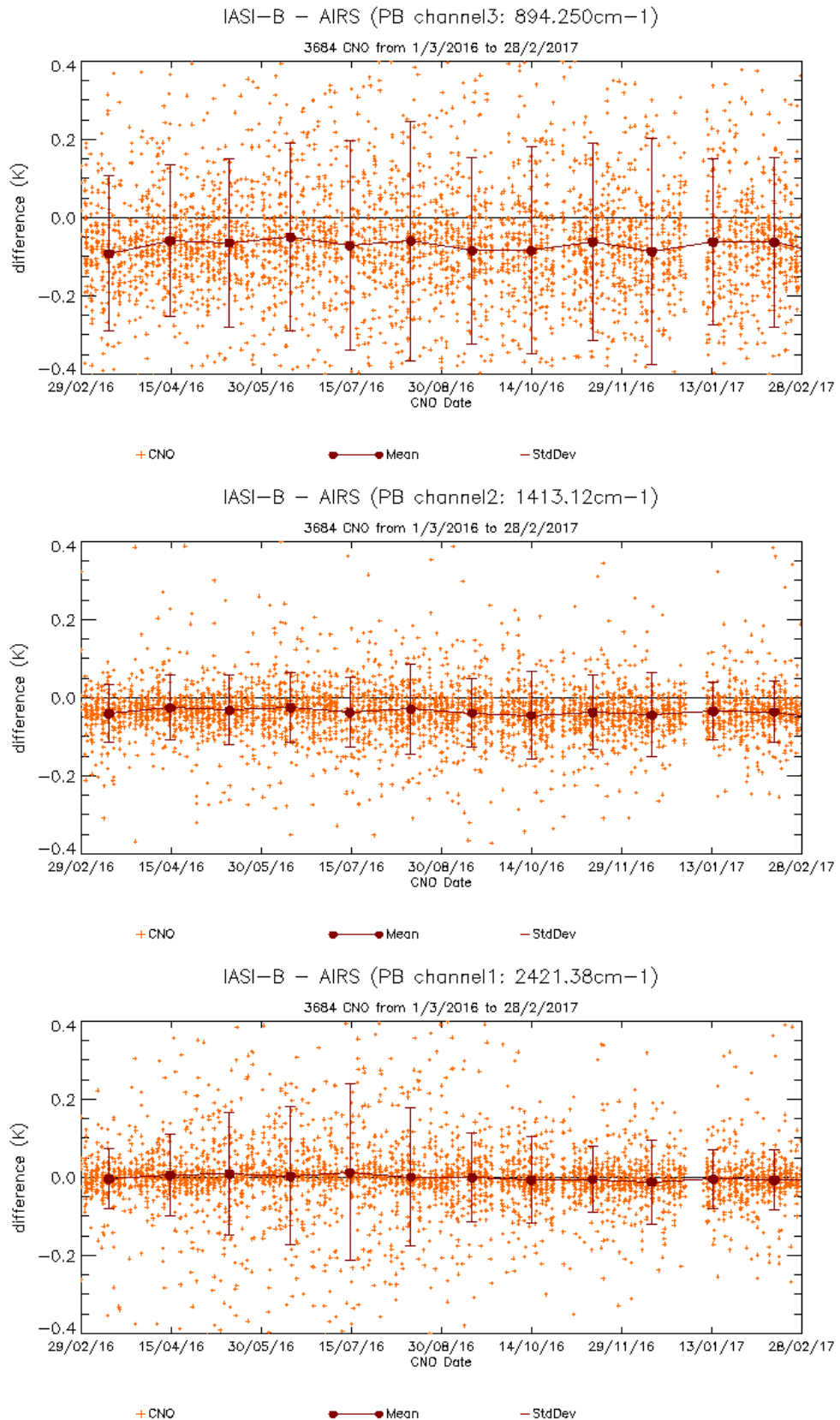


Figure 45 : Temporal evolution of the differences IASI-B – AIRS in brightness temperature over the approximate three IASI bands, with monthly mean.

| | | |
|---|---|---|
|  |  | Doc n°: IA-RP-2000-4332-CNE Issue: 1.0 Date: 2017-07-25 Sheet: 57 Of: 60 |
|---|---|---|

4.9 IIS RADIOMETRIC PERFORMANCES

The main task of IIS is to insure a good relative positioning of IASI sounder pixels with respect to AVHRR. Its performances are studied on one monthly external calibration in three and the monitoring is performed one time a year for REVEX.

4.9.1 IIS Radiometric Noise Monitoring

Refer to REVEX, paragraph 6.9.1.

4.9.2 IIS Radiometric Calibration Monitoring

Refer to REVEX, paragraph 6.9.2.

| | | |
|---|---|---|
|  |  | Doc n°: IA-RP-2000-4332-CNE Issue: 1.0 Date: 2017-07-25 Sheet: 58 Of: 60 |
|---|---|---|

5 IASI TEC SOFTWARE AND INTERFACES

5.1 *IASI TEC EVOLUTION*

A new version “8.7” of the software “TEC” was installed

Table 19 lists previous software evolutions.

| IASI TEC software version | implementation | Comments |
|---------------------------|------------------|--|
| 8.1 | 6 October 2011 | Automatic downloads of L0 products from EUMETSAT FTP |
| 8.2 | 12 April 2012 | New version of product browser (handling IASI L0, L1C products and board configuration). |
| 8.3 | 22 August 2012 | Regularization version before IASI-B CAL/VAL CCAT replaced by CBST in TEC's logs |
| 8.4 | 19 December 2013 | New parameter SP_NV in SLT files Integration of board configuration generation tool (UTOPIE) Integration of LBR products management tool |
| 8.5 | 19 November 2014 | Monitoring of offset voltages from equalization images |
| 8.6 | 1 February 2016 | Detection chain gain and offset optimization Spectral Data Base initialization |
| 8.7 | 8 December 2016 | IHB : radiometric noise from interferograms Scan Mirror Reflectivity computed from L1C (rather than L1A) |

Table 19: IASI TEC at CNES Toulouse

5.2 *SIC EVOLUTION*

A new version “3.5” of the software “SIC” was installed

This Table lists the recent evolutions of the software:

| SIC software version | implementation | Comments |
|----------------------|------------------|--|
| 3.2 | April 2014 | Add of spectral inter-calibration, synthesis tool processed per days, new methods for CNO pre-selection, add of preselection for IASI/AIRS and IASI/CRIS, intercalibration with convolution method for IASI/CRIS |
| 3.3 | April 2015 | New functionalities for data transfer. Improvement of CNO prediction and pre-selection. New parametrization for the synthesis tool. IDL upgrade |
| 3.4 | 23 May 2016 | Additional statistics for the analysis tool |
| 3.5 | 28 February 2017 | Synthesis with PN list |

Table 20: SIC at CNES Toulouse

| | | |
|---|---|---|
|  |  | Doc n°: IA-RP-2000-4332-CNE Issue: 1.0 Date: 2017-07-25 Sheet: 59 Of: 60 |
|---|---|---|

5.3 EUMETCAST INTERFACE

EUMETCast dissemination is used for Near Real Time data reception by IASI TEC at CNES, Toulouse. Each orbit, L1 ENG, L1 VER, and AVHRR 1B products are received under continuous series of 3 minutes PDU. Full dumps are reconstructed by the EUMETCAST terminal and pushed to a IASI TEC server. Since August 2012, NPP/CrIS PDU are also received to perform inter-comparison with IASI.

In case of failure of the prime EUMETCAST station, products remain available several days on a redundant station.

The behaviour of the EUMETCAST reception is nominal.

The following table lists the recent modifications in the EUMETCAST configuration:

| Date | EUMETCAST configuration |
|------------|--|
| 29/03/2011 | End of IASI L0 dissemination via EUMETCAST |
| 03/08/2011 | Hardware and software upgrade of the prime station |
| 04/12/2011 | Hardware and software upgrade of the back-up station |
| 13/07/2012 | Software patch to correct an anomaly concerning AVHHR files (reception of 0 byte files from EUMETCAST) |
| 24/08/2012 | Modification of EUMETCAST configuration to receive NPP/CrIS data |
| 03/2013 | “PARALLEL_RECONSTRUCTIONS” set to 3 to avoid missing PDU problems |
| 09/2013 | “RECONSTRUCTION TIME-OUT” set to 90 to avoid missing PDU problems |
| 09/12/2014 | Antenna repointing and update of reception parameters |
| 21/04/2015 | New SR1 router |
| 10/08/2015 | Replacement of Back-up station HDD |
| 08/2016 | Defective Back-up station (main computer board) : on-going replacement |
| 30/01/2017 | Nominal station : on-going replacement |
| 01/02/2017 | Replacement of Back-up station |

Table 21: EUMETCAST configuration at CNES Toulouse

5.4 FTP INTERFACE

Since March 29th of 2011, IASI L0 full dumps are available in Near Real Time on a EUMETSAT FTP server. The IASI TEC software automatically downloads products from the EUMETSAT FTP server.

The reception of L0 products at IASI TEC is nominal.

| | | |
|---|---|---|
|  |  | Doc n°: IA-RP-2000-4332-CNE Issue: 1.0 Date: 2017-07-25 Sheet: 60 Of: 60 |
|---|---|---|

6 **CONCLUSION AND OPERATIONS FORESEEN**

Please visit <https://iasi.cnes.fr> to get IASI news.

6.1 ***SUMMARY***

The IASI PFM-R instrument is fully operational.

The instrument configuration is the nominal one.

The main events are :

- Moon avoidance on 17-18 December 2016 and on 15-16 January 2017
- In Plane manoeuvre on 29 December 2016 and 1 February 2017
- NormOp to NormOP transition → DPS auto recovery on 15 December 2016
- New TEC software version V8.7 activated on 8 December 2016
- New OPS version V7.4 activated on 25 January 2017
- New SIC software version V3.5 on 28 February 2017

6.2 ***SHORT-TERM EVENTS***

- In Plane manoeuvre on 3 May 2017

6.3 ***OPERATIONS FORESEEN***

- Next decontamination should happen mid 2018
- Next IIS equalization on October 2017
- Update of Scan mirror reflectivity coefficients autumn 2017

End of document